Linkage between the Forest Fires and the Meteorological Parameters during the current climatic regime using Spatial Clustering, Regression, and Combination Matrix Analysis

Manish Pandey[1*], *Aman Arora*[2*], *Masood A Siddiqui*[2], *Satarupa Mitra*[1], *Naveen Pandey*[3], *Sangeeta Soni*[4], *Amanjot Kaur*[5], *U.K. Shukla*[6]

[1]*University Center for Research & Development (UCRD), Chandigarh University, Mohali-140413*
[2]*Department of Geography, Faculty of Natural Sciences, Jamia Millia Islamia, New Delhi-110025*
[3]*School of Environmental Sciences, Jawaharlal Nehru University, New Delhi-110067*
[4]*Jaipur National University, Jaipur-Agra Bypass, Jaipur, Rajasthan 302017*
[5]*Haryana Space Applications Centre (HARSAC), CCS HAU Campus, HISAR- 125004*
[6]*Department of Geology, Faculty of Science, Banaras Hindu University, Varanasi-221005*

*Corresponding Author: *aman.jmi01@gmail.com*, *manish07sep@gmail.com*

Abstract

The present study has been carried out to assess the spatial behaviour of forest fire count (FFC) data and Climate Forecast System Reanalysis (CFSR) derived meteorological parameters in Uttar Pradesh to explore the linkages amongst them. Ten years (2005 to 2014) of forest fire event data and of meteorological data have been analysed using GIS overlay, ordinary least square (OLS) regression, increment ratio (IR) and combination matrix analysis (CMA) to find spatial congruence and causal linkage between FFC and meteorological variables. The results show that approximately 80% of total forest fires occur in March & April only. And, at ten days interval, 65% FFCs were recorded from 21 March to 20 April only. With OLS and IR methods, we found a linkage between FFC and rainfall, relative humidity, solar radiation, and temperature. In contrast, CMA indicated a periodicity in the FFCs of the highest category.

Keywords: *Forest Fire – meteorology linkage, Overlay Analysis, Ordinary least square regression, Combination matrix analysis, CFSR, Uttar Pradesh*

Introduction

Forest fire is the worldwide phenomenon affecting forest structure, composition, plant species redistribution, etc. (Randerson et al., 2006; Bowman et al., 2009). During the last couple of decades, increase in the number and intensity of forest fire at an alarming level on all vegetative continents have raised the question on control and mitigation of this anthroponatural phenomenon and our incomplete understanding of causes, effects, and feedbacks of fires (Flannigan *et al.* 2000, Westerling 2006). Though forest fires have been thought to be linked to changing climatic scenarios over the globe, and the linkage between what causes increased forest fire activities and changing climate and vice versa have been under continuous inquiry (Flannigan *et al.* 2000). Still, the need to study the causal relationship between weather elements and components of a forest fire at regional to local levels in changing climate scenarios is required to understand the causal linkage better. Forest fire ignitions are either set by natural phenomena like lightning (Krawchuk *et al.* 2006, Renkin & Despain 1992), volcanic eruptions (Ainsworth & Boone Kauffman 2008), vegetation cover and topography (Kanevski and Pereira 2017), and anthropogenic drivers like forest clearing (Nepstad *et al.* 2008, Cochrane 2003), population pressure (Laurance *et al.* 2001, Beniston 2003), population density and socioeconomic activity (Westerling 2016). This further need for a study of "climate - forest-fire" linkage is evident from the even very recent researches in the field of pyrogeography (Read *et al.* 2018, Conedera *et al.* 2018). For example, Flannigan et al., (2013) suggest that increasing boreal forest fires may not be accelerating climate warming. However, several studies indicate a correlation between increasing fire events and changing climatic parameters (Bradstock 2010, Liu & Wimberly 2016, and references therein). The study by Hernandez *et al.* (2015) vindicates "strong control of the wildfire activity by the concomitant weather" and leaves no doubt about the relationship between fire activity and weather elements. A large number of researches establishing linkage between meteorological parameters and various components of forest fire regime (Flannigan & Harrington 1988, Stocks *et al.* 2002). Still, there are studies like the one by Flannigan *et al.* (2013) which reinstates and revokes the need to reinvestigate the climate-forest-fire relationship further. The relationship of various parameters of climate and forest fire is performed using different components of forest fire regime as the independent variables.

Forest fires have been widely occurring in almost all the vegetation-covered regions of India (Joseph et al. 2009). Total carbon storage in Indian forests has been estimated to in 1.9-4.1 PgC (Ravindranath, *et al.* 1997). It is being noticed that fire events have been increasingly recorded in the forested areas with fluctuating climatic parameters at different temporal scales. Ahmad and Goparaju (2018) have presented an analysis of forest fire and climatic parameters at different temporal scales in the state of Odisha, India and found significant relationship between climate events and meteorological parameters. Most of forest fire studies in different parts of India have focused on fire frequencies, fire coverage and the correlation between meteorological parameters and fire frequencies, fire risk assessments and their modelling (Habib *et al.* 2006, Badarinath *et al.* 2011, Ahmad & Goparaju 2017, Prasad *et al.* 2008, Joseph *et al.* 2009, Kiran Chand *et al.* 2006, Kodandapani *et al.* 2004, Chand *et al.* 2007, Jaiswal *et al.* 2002, Erten *et al.* 1996). Even with the forest fire studies focussing on different parts of India, the fires and its relationship with various meteorological parameters' fluctuations are poorly understood and no studies have been found which attempted to explore this relationship in some parts of the highly vegetated regions like Uttarakhand and Uttar.

Despite long held appreciation of forest fire and anthropoclimatic relation with flammability at global as well as local scales, global forest fire activities have started to only been revealed during 1980s with the *global coverage of satellite observa*tions (Arino et al. 1999). The advancement in satellite data technology has provided earth science communities working in the field of pyrography with a set of satellite data products viz. ATSR-2, MODIS fire products, CALIPSO, AVHRR fire products, etc. (Tansey *et al.* 2008, Nogueira *et al.* 2017, Kahiu & Hanan 2018, Laurent *et al.* 2018). The pyro-satellite products and technology are still in advancement phase and are being modified in order to achieve "near real time fire alarm information system" using satellite products and models.

The present study aims at:

1) spatially analysing forest fire count (FFC)/density (FFD) at annual, seasonal, and 10-day intervals to work out the fraction of the forest fire season during which different categories of FFCs occur; 2) assessing the trend of different meteorological parameters viz. temperature, rainfall, relative humidity, and solar radiation at the same 10-day interval and find out any trend in spatial congruence of the FFC/ or FFD clustering (spatial congruence can be defined in terms of geometrical overlaying of the areas of one parameter over another, here in this study, area of high FFC and different meteorological

parameters); and 3) finding out relationship (if any) between different meteorological parameters and forest fire frequencies, in Uttar Pradesh state of India.

Study Area

The state of Uttar Pradesh has been selected for the study of forest fire events starting from 2005 to 2016 because no studies connecting FFCs and meteorological parameters have been conducted here (see figure 1). Areal coverage wise, Uttar Pradesh (total area of 243290 km2) is India's fourth-largest state. Situated on the northern spout of India, it shares its northern international boundary with Nepal. The Himalayas border the state on the north, but the plains that cover most of the state are distinctly different from those high mountains. It lies between latitude 23°52'8.71"N to 30°24'44.60"N and longitude 77°25'52.28"E to 84°40'25.14"E. Uttar Pradesh has a humid subtropical climate and experiences four seasons. The winter in January and February is followed by summer between March and May and the monsoon season between June and September, the autumn season fall between October and December. In 2011 the recorded forest area in the state was 16,583 km^2 which is about 6.88% of the state's geographical area (Forest Survey of India, Ministry of Environment & Forests, Government of India, 2012). Almost all of these forested areas confine themselves to parts of the state with low annual rainfall (50–70 cm), a mean annual temperature of 25–27 °C and low humidity.

The state has 1,626 km^2 under very dense forest, 4,559 km^2 under moderately dense forest and 8,153 km^2 of area under open forest (ISFR 2011, Govt. of India). Main vegetation types of this region are Tropical Moist Deciduous Forest, Tropical Semi-Evergreen Forest, Dry Deciduous Forest and Swamp and Riparian Forest As per the satellite data derived land use/ land cover (LULC) data, Uttar Pradesh, as of October-December 2015, hosts about 14,679 km^2, 6.09% of its geographical area, as forest cover. In terms of forest canopy density classes, the state has 2,617 km^2 (26.78%) under very dense forest, 4,069 km^2 (32.90%) under moderately dense forest and 7,993 km^2 (40.32%) under open forest (see supplementary figure 3). Areas with most of the forest cover, delineated as forest clusters and designated as A to E (see supplementary figure 2) have been selected for analysing the linkages between forest fire and meteorological parameters. The forest cover percentage share in different districts of the study area (see figure 3b) has helped to delineate the clusters.

Materials and Methods

Database

In the present study, two types of data have been used. The first data is the forest fire count (FFC) data acquired from Forest Survey of India (http://fsi.nic.in/forest-fire.php), second data is the meteorological CFSR data (daily time series) in comma separated values (.csv) file format which was downloaded from the NCEP (globalweather.tamu.edu). These two datasets have been imported into GIS environment and overlaid to the state and district boundaries downloaded from DIVA-GIS (http://www.diva-gis.org/Data). A brief discussion of the characteristics of all data sets used is presented below.

Forest Fire Data

We have acquired FFC stored in MS-Excel (.xls file) format for the 11-year period starting from 2005 to 2016. The data obtained from Forest Survey of India (FSI), Ministry of Environment, Forest and Climate Change (MoEFCC), Govt. of India incorporates a number of information related to forest fire events including: 1) fire event date; 2) locational information in terms of latitude and longitude; and 3) Survey of India toposheet number in which that fire event occurred. The locational information available in the data sheets helped to convert the fire data into vector file. For the present study area, the FFC provided on the FSI Portal is available for the period 1995 to 2016, but the meteorological data used in this study is available only up to 2014. The fire data set before 2005 shows two characteristics viz. a) very few fire events recorded during the period 1995 to 2004, and b) inconsistency in data records, hence we chose to truncate the forest fire data from 2005 to a maximum up to 2014 for this study. FFC data distribution at yearly, monthly, (see figure 4a & 4b) and at 10-day interval has been used (see figure 5) for spatial appraisal of fire events and how FFCs change over time in the study area.

Meteorological Data

The CFSR data, developed at the National Center for Environmental Prediction (NCEP), an American centre working under the National Oceanic and Atmospheric Administration (NOAA), delivers national and global weather, water, climate and space weather guidance, forecasts, warnings and analyses for the various Partners and External User Communities. According to Saha et al., (2014), the revised CFSR data includes certain enhanced and new features like (i) the guess fields at 6-h forecast from a coupled atmosphere-ocean climate system which also has an interactive sea ice component; (2) a higher horizontal resolution (~38 km) for the atmosphere as compared to its previous atmospheric reanalyses dataset; and (3) assimilation of satellite radiances instead of retrieved temperature as well as humidity values. The CFSR is also enhanced using the observed greenhouse gas (GHG) concentrations, aerosols, solar variations; and assimilates hydrological values from a parallel land surface model derived by forcing the Climate Prediction Center (CPC) from NOAA's closely confined rainfall analysis (Xie et al. 2010).

The CFSR daily data have been acquired in the .csv file format from Global Weather Data for SWAT portal (http://globalweather.tamu.edu). The meteorological parameters extracted from the CFSR data used in this study include: 1) Temperature (in $^{\circ}$C), 2) rainfall (in cm), 3) relative humidity (fraction), and 4) solar radiation (MJ/m^2). A total of 11 year (2005 to 2014) data for 226 weather stations (Table no. 01) of CFSR covers the entire study area. The CFSR data acquired in .csv file format have also been exported to vector file format (.shp file format) for geospatial assessment of all the meteorological parameters. All the CFSR data files were available station wise and we have downloaded data for 226 stations. The downloaded files for all 226 stations were clumped into one file using query with station IDs and meteorological parameters. The clumping algorithm was performed with a python script illustrated in the figure (2). This combined dataset was used as kriging interpolation input to have spatial appreciation of all the meteorological variables over the entire study area. The meteorological parameters have also been interpolated spatially, at 10-day intervals and are shown in figures 6(a - d). For better understanding of monthly and yearly trend, the graphs presented in figures 7 (A – D) has been prepared.

GIS Data

The zero level to second level of administrative divisions has been used in the present study. Administratively, the GIS vector data used was up to second level i.e. district-level boundaries to match the forest fire data levels which was also available up to district level. The first and second level GIS data was downloaded from DIVA GIS (http://www.diva-gis.org/Data) and was further validated and updated with details obtained from Census of India atlas of year 2011 (http://censusindia.gov.in/2011-Common/CensusData2011.html). Forest cover and vegetation type data were acquired freely from Open Street Map Portal (https://www.openstreetmap.org/) and Forest Survey of India Report 2017 for Uttar Pradesh (http://fsi.nic.in/isfr2017/uttar-pradesh-isfr-2017.pdf). Forest cover distribution in the study area is shown in the supplementary figure (2) and district wise forest coverage is presented in figure (3b).

Methodology

Data Preprocessing

At first, the bulky CFSR data was simplified using the Python script (see figure 2), so that it can be analysed further in GIS and statistical environments. The program selects the variables from a single data on basis of provided keywords common to all the data files in the script and runs the loop till all the data in the last file is stored and arranged in one single file as per the script code. Two of the common parameters available and selected from among all the files are data type and location. The script has utilized the Panda platform which is an open source software package comprising of BSD-licensed library and provides high-performance, easy-to-use data structures and data analysis tools for the Python programming, for analyse and finalize the data. It is a powerful and flexible toolkit to perform data analysis / manipulation (McKinney and Team 2015).

The GIS data used here have been projected with the following specification listed in the table (1).

Spatial Pattern Analysis using GIS Overlay Approach

The CFSR datasets and forest fire points were visualized and spatially analysed with different approaches and techniques in ArcGIS software package. Forest fire density (FFD) was computed from the FFC data using the formula presented in equation (1):

$$FFD = \frac{Total\ forest\ fire\ counts\ during\ 2005{-}2014\ in\ a\ district}{Total\ forest\ cover\ area\ of\ the\ district\ in\ 2015} \qquad \textit{(Equation. 1)}$$

Since FFC and FFD data have shown to reveal the same ordering pattern of areas delineated by clusters B, E, and A which have covered most of the forest cover in the study area, except inverse ordering pattern for sparse, less forested clusters viz. clusters C and D, we have used FFC data for GIS and statistical analyses in our pursuit of finding linkage (see tables 2 and 3). To analyse the spatial pattern of forest fire events, the point density tool of spatial analyst toolbox was utilized while for showing the trend of meteorological parameters the kriging interpolation technique of the same toolbox was used. Kriging is a regression technique used in geostatistics to approximate or interpolate data and is also used in reproducing kernel methods e.g. splines and support vector machines. The ordinary kriging (OK) works as per the following equation (2):

$$\hat{Z}(S_0) = \sum_{i=1}^{N} \lambda_i Z\,(S_i) \qquad \textit{(Equation. 2)}$$

where $Z(S_i)$ is the measured value of different parameters used at the ith location, λ_i is an unknown weight for the measured value at the ith location, S_0 is the prediction location, and N is the number of measured values. The OK in the ArcMap 10.3 version's Spatial Analyst Tool works based on method developed by Cressie, (1992).

Finally, the forest fire count (FFC) vector information was visually overlaid to the meteorological parameters vector data to assess the spatial pattern of clusters of low and high values fractionated at 10-day temporal interval in order to see the of relationship among all the independent meteorological variables to the forest fire variable. Overlay algorithm is a GIS operation that is performed by superimposing multiple vector as well as raster data layers (representing different themes) together over one another for the purpose of identifying relationships between them. An overlay presents a composite picture of the story by combining the geometry and attributes of the input data sets. The basic principles working in this operation are identity, intersect, symmetrical difference, algebraic union and geometry updation.

Statistical Analysis

In order to find relationship between forest fire density (FFD) and meteorological variables, Ordinary Least Squares (OLS) regression has been used which is one of the standard methods to assess the relationship between a dependent variable and a group of independent variables. The OLS works based on the equation (3) expressed as:

$$Y = \beta_0 + \sum_{j=1}^{p} \beta_j X_j + e \qquad \textit{(Equation.3)}$$

Where Y is the dependent variable, β_0, is the intercept of the model, X_j corresponds to the jth explanatory variable of the model (*j= 1* to *p*), and *e* is the random error with expectation 0 and variance σ^2. After running the model, it has been examined from 6 perspectives: 1) model performance, 2) each explanatory variable behaviour, 3) model significance, 4) stationarity, 5) model bias, and 6) spatial autocorrelation or Moran's I statistics as it's been suggested by Getis & Griffith, (2002) and Shumway & Stoffer, (2006) the results for which are explained in the results and discussion section.

Lastly, we have computed annual increment in the meteorological parameters to see whether any logical pattern in relationship is found between the forest fire density per annum and incremental values of each meteorological parameter. For computation of percentage annual increment in values of met parameters, we have applied the formula expressed by equation (4):

$$IR = \frac{(X_t - X_{t-1})}{X_{t-1}} \times 100 \qquad \textit{(Equation. 4)}$$

where $IR = Increment\ Rate\ (in\ \%)$, $X_t = \ Value\ of\ met\ parameter\ of\ the\ year\ (t)$ and $X_{t-1} = Value\ of\ the\ met\ parameter\ of\ the\ preceding\ year\ (t-1)$

Percentage *IR* values of all the met parameters for entire 11 year period (2005-2014) were plotted with relation to the forest fire count data (see figure 8 and supplementary table 3).

Choosing the Most Appropriate Trendline

For finding the most appropriate trend in the forest fire and meteorological data in order to see the relationship, we relied on getting a trendline of the FFC/or FFD as well as met parameters which shows most reliable data trend with the R-squared value approaching 1 or near 1 (Hales et al., 1999; Grassini et al., 2013; Posavec et al., 2006). Most of the forest fire or meteorological data used were best fit with polynomial function with 2 or more orders (see figures 3a, 3b, and 7A to 7D). A polynomial trendline is a curved line that is used when data fluctuates (Paniello et al. 2011). The order at which the polynomial function best fits determines the fluctuations in the dataset i.e. how many bends (hills and valleys) appear in the curve best fit trendline are representative of polynomial order. A second order polynomial, for example, trendline generally has only one hill or valley, a third order polynomial function generally displays one or two hills or valleys and next orders follow the same suite. This method helps to compare the trend of rising or falling behaviour of values of FFC/ FFD and met parameters over the study period.

Combination Matrix Analysis (CMA)

The combination matrix analysis method is used in many fields of research to deduce possible combination of linked parameters and helps in classification. There are two types of CMA: 1) quantitative CMA; and 2) CMA qualitative. Quantitative CMA is a mathematical technique which helps to identify which possible combination of independent variables are related to specific value range of dependent variables and helps in permutation-combination analyses. Qualitative CMA is the method of finding out best suited combinations of independent variables to the corresponding dependent variable and is frequently used in classification studies and probability functions. There are studies which have used descriptive or qualitative as well as non-descriptive or quantitative CMA techniques depending upon their objectives (Deumlich *et al.* 2006, Lasaponara *et al.* 2004, Murthy *et al.* 2016, de Araújo *et al.* 2012) . We have applied CMA descriptive/qualitative methods for five forest cover distribution clusters selected for analysing the FFC classes and associated meteorological parameter combinations by using combination matrix method used by Thackway *et al.* (2008), Ferreira (2000), and Becerril-Piña *et al.* (2015). Like Ferreira (2000) and Said Guettouche & Derias (2013), we have sorted combinations of meteorological conditions associated to each class of FFC categories for each cluster of forested areas. For each FFC class (see table 2 for values of different FFC and meteorological parameters classes used in derivation of combination matrix), different cluster-representative meteorological values are set. An arrangement of all set of values of different parameters (meteorological parameters here) associated with a parameter (FFC here) is defined as combination matrix in this work. Different set of meteorological parameters associated with different classes of FFD for each cluster is given in supplementary table (2a to e) (given as supplementary table 2). This method also helped to delimit the fire seasonality peak periods and its associated meteorological parameter combinations.

Result and Discussion

Forest Cover and Forest Fire Count (FFC)/Density (FFD) Distribution

GIS overlay analysis has helped to delineate 5 clusters of most forest coverage in congruence with most of the FFCs in the study area have been recorded by the Forest Survey of India (FSI). The clusters have been designated as A, B, C, D, and E (see supplementary figure 2). In an attempt to find out spatial congruence, we first looked for cluster wise areas studded with forest covers. And this work shows that Cluster-B has largest coverage of forest (48503km^2), with 20694 km^2 of forest coverage, Cluster-E stands at the second. Clusters D (17772 km^2), A (12258 km^2) and C (10709 km^2) stood on third fourth and fifth rankings respectively (supplementary figure 2 and tables 3 and 4). Price & Bradstock (2014) have found that larger the vegetated to non-vegetated ratio in an area, the larger is the possibility for a large number of fire event counts. This relationship has been found valid in our study area in clusters (B, E and A) with maximum forest cover and larger forest fire counts. Exceptions to this may be because of other factors like dominant vegetation type, other social, economic, cultural and topographic drivers triggering fire events in clusters C and D.

Lakheempur Kheri is the district with maximum recorded forest fires from 2004 to 2015. Sonbhadra and Pilibhit are placed on second and third place respectively after Kheri in terms of recorded forest fires. Lakheempur Kheri, also, stands on first place for the maximum share (3.19%) of forest cover in the state following by Sonbhadra (2.87%), Hardoi (2.48%)

and Sitapur (2.38%). Cluster wise, the FFC recorded in the study area are given in the table (2) along with the corresponding forest coverage in each cluster. We found that except for cluster D, the FFC values are highest in clusters with highest FC areas and the same it found to be true in case of lowest values of FFC/FFD and FC (see tables 2 & 3) which maybe because of non-linearity in the relationship between FFD and FC variables as well as human set fire ignition triggers which depend upon a number of social, cultural, economic and other factors (Ganteaume *et al.* 2013, You *et al.* 2017). The clusters with the highest FFD classes are characterized mostly by tropical dry deciduous forest cover which provide ideal fire fuel type susceptible to fire events because of higher flammability of vegetation type (Nunes *et al.* 2005, Biswas *et al.* 2015). Different vegetation types show different flammability (Bond & van Wilgen 1996, Uhl & Kauffman 2012, Fares *et al.* 2017). The vegetation classes in this study area in clusters B and E are corroborating that relationship of vegetation and fire characteristics. Though, this relationship becomes complex when it is examined in case of FFC pattern in clusters A, C and D. Change in land cover may also be responsible for change in FCC behaviour in the study area resulting into exception in congruity of areas with forest cover *vis-à-vis* forest fire counts. The order of FFC (table 2) appears to be in the order of flammability of vegetation cover types in each cluster, except for cluster D, though, there is need to fractionate and quantify percentage coverage of each vegetation type in the study area which was not in the scope of this work's objectives and it requires further inquiry.

Forest Fire Count/Density and Meteorological Parameters

Forest fire density, fire events per unit area, as per definition by Ganteaume and Long-Fournel, (2015), has been computed in ArcGIS 10.3 in GIS environment and been found to vary over the study period at different temporal scales of yearly, monthly and at 10 days interval. It is found that the FFC and FFD both show the same order of correlation in highly forested clusters B, E and A (table 3), except clusters C and D which are sparse and less dense in terms of forest cover, using fire count data instead of fire density data makes no difference as for as relation between the set of meteorological variables and fire is concerned. Hence, we have compared the FFC data patterns with those of meteorological parameters in this study. At the fourth polynomial order, the forest fire count and density data since 2005 to 2016, the trendline shows first increasing (from

2005 to 2010) and then decreasing trend (from 2010 to 2015) with R^2 value 0.37. This R^2 value indicates acceptable strength in the relationship between the two plotted variables (Meng and Meentemeyer 2011).

The meteorological data shows no trend when plotted on linear or logarithmic scales over time during the entire 11 year period (2005-2016). Whereas T, RH, and SR show best fit with second order of polynomials for which R^2 value reaches approximately to one (see the figures 7A to 7D) but the rainfall (P) does not show best fit with second order polynomials. But at 5th order, the best fit line for annual rainfall and annual FFC data show R^2 value to about one (see figures 4a and 4b). Getting the best fit lines for which R^2 value reaches near one is significant for prediction of trend in distribution of a parameter (Microsoft® 2016).

The figures 6a to 6d display a complex relationship between distribution of meteorological parameters and forest fires. The areas with high relative humidity (figure 6c), high rainfall (figure 6a), low temperature (figure 6b), and low solar radiation (figure 6d) should show high rainfall but because of the interplay of many other non-meteorological factors, the relationship in the above variables does not appear to be as straight forward as is seen in the maps. But the forest fire count map (figure 4b) does show an increasing monthly trend between March to May during the entire study period and the trend follows the same as seen in case of monthly meteorological parameters (see figures 4a and 4b). This increasing trend of forest fire and meteorological parameters does show a temporal congruity of FFC and meteorological parameters indicating a functional linkage among them.

Despite irregularity in the behaviour of forest fire events and rainfall trend at annual scale over the study period, we find (figures 4a & 4b) that there is first a generally increasing trend in forest fire events and rainfall events and then decreasing trend with some years of exception. This implies that there is a relationship between forest fire events and rainfall events.

Statistical Analysis of FFC and Meteorological Parameters

In order to find out to what extent meteorological parameters help in providing suitable ambience for forest fires events to occur, OLS regression analysis was performed and the results of the analysis show moderately significant relationship between dependent variable (FFC) and independent variables (rainfall, temperature, relative humidity, solar radiation). Model performance was evaluated based on values of multiple R^2 and adjusted R^2. The values of multiple R^2 (0.279156) and adjusted R^2 (0.235468) indicate that the OLS model explains only about 24% story of relationship of dependent variable (FFC) and explaining independent meteorological variables. This may be because of a very large number of non-forested areas also (where fire events have been recorded by Forest Survey of India) been used as input in this analysis as well as many human drivers controlling the forest fire occurrences (Mancini et al. 2018). Mancini et al., (2018) points out six human drivers directly (or indirectly) triggering forest pyrographic events viz. 1) landscape and land-use, 2) agriculture, 3) income and wealth, 4) population, 5) education, and 6) job market. The other factors affecting forest fire events other than meteorological parameters, not being considered in this analysis, may also be responsible for not very strong statistical performance of the model. The coefficients for each independent/explanatory variable reflect that there is found a moderate relationship between dependent variable (FFC) and explanatory/independent variables. We found positive relationship between FFC and solar radiation (SR) but negative relationship between FFC and rainfall (P), temperature (T), as well as relative humidity (RH). Variable Inflation Factor (VIF), which explains redundancy among independent variables, indicates that there is no redundancy in the variables chosen to model the relationship as all the VIF values are less than 7.5 (Graeme D. Hutcheson 1999). T-statistics coupled with p-values for each explanatory variables (see the model summery in the appendix-Model Output Report) suggests that among the explanatory variables, T (StdError: 0.035830; t-stats: -3.762148; p-value: 0.000364*) and SR (StdError: 0.060527; t-stats: - 4.010910; p-value: 0.000159*) are statistically significant. Cyr *et al.* (2007) state that in coniferous boreal forests of Canada, there has been found a significant relationship between solar radiation and forest fire frequency as they found that slopes exposed to more direct solar radiation and prevailing winds show more vulnerability to fire) whereas R and RH do not perform statistically significant roles in the model. Not very statistically strong relation between FFC and rainfall (R) and relative humidity (RH) in our study and significant relation between these two same (R, RH) parameters and forest fire in study by Jupp *et al.* (2006) in terms of revelation of a “convincing, quantitative link between the number of fire scars and regional variability in early summer rainfall” supports the view that fire ignition in our study area is human set and there is need of more forest fire modelling attempts including social, economic, cultural, topographic variables. This non-natural ignition of fire events in the area is confirmed by reports in the newspapers reported from the area (IANS 2016). Statistically non-significant Koenker (BP) statistic (Koenker (BP) stats 6.290834; Prob (>chi-squared), (4) degrees of freedom: 0.178456) suggests that explanatory variables are, though moderately, associated to the changes in independent variable. Gillett *et al.* (2004) have found positive relation between rising temperature and forest fire burned area but how significantly and to what extent temperature affects the fire phenomena have not been in their agenda of research. Since, in our study, Koenker (BP) statistic is not statistically significant (see the supplementary file Appendix C OLS Output Report), Joint F-statistics (Joint F-stats: 6.389834; Prob (>F), (4.66) degrees of freedom: 0.000208*) but not the Joint Wald Statistics (Joint Wald Statistic: 18.088362; Prob (>chi-squared), (4) degrees of freedom: 0.001186*) is to be consulted. The Koenker (BP) Statistic which is used to determine whether the explanatory variables in the model have a consistent relationship to the dependent variable both in geographic space and in data space suggest that the model used here is not stationary. Non-stationarity of the model means that the change in R, T, RH, and SR does not lead to linear change in FFC the same way everywhere spatially and over dataspace. The model bias assessed with the help of Jarque-Bera statistic (Jarque-Bera Statistic: 83.773048; Prob (>chi-squared), (2) degrees of freedom: 0.000000*) and spatial autocorrelation analysis (see the supplementary file named Moran’s-I-Residuals) rightly point out that the model has certain level of bias. The model bias may result from a variety of factors including omission of some very important independent variables and non-linearity of relationship among dependent and explanatory variables. In the study area, almost all the forest fires are anthropogenically set, and there are several human-societal, cultural, and economic variables which are not part of this investigation, and including these variables in the future researches may decrease the model bias and improve its performance as the studies by Graeme D.

Hutcheson, (1999); Mann et al., (2016); and Van Der Werf et al.,(2008). Mancini et al., (2018) put emphasis on inclusion of human related parameters in pyrogeographic investigation in order to have better understanding of fire events. With the only four natural parameters used here in the study and not including any human related variables warrants further mulling about inclusion of natural and human-social-economic-cultural parameters to incorporate in studies seeking statistical modelling the linkage between FFC and it driving/triggering parameters in future researches.

After finding a moderate statistically significant relationship among FFC and meteorological parameters, analysis of increment ratio (IR) of forest fire count for three months viz. March, April, and May for each year and for the met parameters for the same three months provides insight into the relationship between FFC and meteorological parameters in our study area (the computation of IR is discussed in detail in methodology section). The results of IC analysis presented in figure (8) suggests that forest fire events are inversely related to rainfall (R) and relative humidity (RH) whereas temperature (T) and solar radiation (SR) are positively, though weakly, correlated to forest fire events. The negative relationship between forest fire activity and rainfall, which has not been found statistically very significant and which is widely reported by many workers in different climatic and topographic setting from the world over (Chen *et al.* 2014, Nogueira *et al.* 2017, Fox *et al.* 2015) has been found to be the valid linkage between the two through IR method. The behaviour of relative humidity and forest fire in the graph (see figure 8) also indicates the inverse relation between the two. Read *et al.* (2018) have, through their modelling approach linking lightning and fire ignition, reported that "weather properties such as temperature, relative humidity, wind speed and rainfall can affect all parts of the lightning ignitions process" and hence there is a, though indirect, relationship between forest fire phenomena and relative humidity.

Combination Matrix Analysis (CMA)

The construction of combination matrix based on methods used by Said Guettouche & Derias (2013), Ferreira (2000), Becerril-Piña *et al.* (2015), Sujatha & Rajamanickam (2015) has helped to classify different categories of FFC associated with the meteorological parameters which characterized those classes of fire events (see table). The CMA results indicate that out of total FFC events, 60% could have been of very low (VL_{FFC}) category, 22.86% of forest fire events could have been identified to be of low (L_{FFC}) category, and medium (M_{FFC}), high (H_{FFC}), and very high (VH_{FFC}) categories accounted 17.14% cumulatively. Individually, each of the M_{FFC}, H_{FFC}, and VH_{FFC} categories constituted 5.72 %, respectively, of the total FFC events during the entire 11 year (2005-2016) period (see table 2). The MCA also helped us to identify the set of meteorological characteristics associated with different categories of FFC events. This helped to find generalization of FFC- met parameter association. Ruosteenoja & Räisänen (2013) found out that sunny weather and low RH most likely favour a risk for forest fire ignition. Inverse relationship between solar relative humidity and solar radiation (Swartman and Ogunlade 1967) suggests the risk of high forest fire probability. The conditions in the study area favouring VH_{FFC} and associated meteorological parameters (VL_R-L_R, H_T- H_T, L_{RH}- L_{RH}, M_{SR}-H_{SR}) are behaving according to this general rule. During the low rainfall conditions, there are more probable risks of forest fire ignition or forest fire expansion (Castillo Soto 2012). Both of our forest fire hot spots, represented by clusters B and E (see supplementary figure 2), hosting FFCs of M_{FFC}, H_{FFC} and VH_{FFC} events corroborate, with few exceptions, the relational linkage between FFCs and favourable meteorological conditions (Westerling 2006; Pechony and Shindell 2010; Chen et al. 2014). The exception to the general rule of fire-rainfall relation i.e. occurrence of H_{FFC} events during the conditions of high rainfall in cluster B are related to high altitude and ruggedness of the area; and are because the meteorological conditions in high mountainous areas, cluster B, differ from those of the low altitude areas, like in cluster E. The reported general rule of low rainfall conditions favouring the risk of high forest fire ignition and expansion still holds good in cluster E. The variability in relationship between set of meteorological variables and FFC may be suggestive of involvement of forest fire drivers other than meteorological factors. The 60% share of FFCs of VL and 22.86 % FFCs of L category, cumulatively constituting more than 82% of total FFCs, explains the statistical model bias and low to moderate performance of the OLS model.

CMA also helped to fractionate forest fire season into different area and time specific FFC intensive periods. In other words, it (CMA) helped to find cyclicity or episodic nature of forest fire events of a particular class of FFC during a particular time period during the

11 year study period. It is notable that FFCs of VH and H category have been found to occur during the 21st March to 10th April time interval in Clusters B and E. The FFCs of VH category occurred in cluster B during the same time period only. FFC events of very-low, low, and medium appear to occur in varying meteorological conditions having no definite set of favourable set of meteorological conditions (see table 6). From the combination matrix, it is clear that the fire events falling in the very high category of FFC are occurring under set of meteorological conditions which, in theory, are to be favourable to induce/support fire events. For instance, high to very high temperatures, low to no rainfall, low relative humidity and high to very high solar radiation combinations produce conditions conducive to fire events (Byram and Jemison 1943). Areas with higher forest coverage appear to have association with the higher forest fire density/ forest fire count in our study area but we did not find any literature supporting this relationship. There are, though, some studies which found relation of forest cover loss rates with the forest fire frequencies (Pinchot 2011; Fanin and van der Werf 2015).

Conclusion and Recommendations

We, in the present study, found that observation of forest fire events of highest classes and those of meteorological parameters are spatially congruent to a significant extent. That is, areas with high FFC category have occurred in areas with high forest coverage which implies that there is linkage between forest fire events of a particular FFC class and set of favourable meteorological parameters. Combination matrix analysis does suggest that the cyclicity of FFC events of highest class is found to occur during a specific time period of the year during (21st March to 10th April) the entire study period; and those particular classes of M, H and VH FFC events are suggestive of their occurrence during only a particular set of met parameters. FFC events of very low to medium class do not seem to occur with particular set of met parameters indicating their week relationship to the met parameters. Statistical modelling of the FFC and only four met parameters viz. R, T, RH, and SR shows only moderately promising statistical results and show bias in the modelling suggesting inclusion of many other human, social, economic, cultural parameters to reassess the relationship in the study area in future researches.

Acknowledgement

Authors are grateful to the School of Environmental Sciences, Jawaharlal Nehru University, New Delhi, for providing their lab facility to carry out the GIS and statistical analyses in ArcGIS software. There is no conflict of interest among authors of this MS.

Ethical Statement

The MS has been prepared following all the ethical standards needed to publish research articles in SCI; Scopus indexed journals with high repute. There is no conflict of interest among the authors and all of them have given their ethical approval for this MS. Each one involved in working/preparing for this work has provided their consent regarding this MS' communication to the Journal of Geovisualization and Spatial Analysis.

Grant Information

No grant from any agency has been used in this work.

References

Ahmad F, Goparaju L (2018) A geospatial analysis of climate variability and its impact on forest fire: a case study in Orissa state of India. Spat Inf Res. doi: 10.1007/s41324-018-0197-8

Ahmad F, Goparaju L (2017) Geospatial Assessment of Forest Fires in Jharkhand (India). Indian J Sci Technol 10:1–7. doi: 10.17485/ijst/2017/v10i21/113215

Ainsworth A, Boone Kauffman J (2008) Response of native Hawaiian woody species to lava-ignited wildfires in tropical forests and shrublands. For. Ecol. Springer Netherlands, Dordrecht, pp 197–209

Arino O, Rosaz JM, Goloub P (1999) The ATSR World Fire Atlas- A synergy with'Polder' aerosol products. Earth Obs Q 64:1–6.

Badarinath KVS, Sharma AR, Kharol SK (2011) Forest fire monitoring and burnt area mapping using satellite data: a study over the forest region of Kerala State, India. Int J Remote Sens 32:85–102. doi: 10.1080/01431160903439890

Becerril-Piña R, Mastachi-Loza CA, González-Sosa E, et al. (2015) Assessing desertification risk in the semi-arid highlands of central Mexico. J Arid Environ 120:4–13. doi: 10.1016/j.jaridenv.2015.04.006

Beniston M (2003) Climatic Change in Mountain Regions: A Review of Possible Impacts. pp 5–31

Biswas S, Vadrevu KP, Lwin ZM, et al. (2015) Factors Controlling Vegetation Fires in Protected and Non-Protected Areas of Myanmar. PLoS One 10:e0124346. doi: 10.1371/journal.pone.0124346

Bond WJ, van Wilgen BW (1996) Fire and Plants. doi: 10.1007/978-94-009-1499-5

Boschetti L, Eva HD, Brivio PA, Grégoire JM (2004) Lessons to be learned from the comparison of three satellite-derived biomass burning products. Geophys Res Lett 31:n/a-n/a. doi: 10.1029/2004GL021229

Bowman DMJS, Balch JK, Artaxo P, et al. (2009) Fire in the Earth System. Science (80-) 324:481–484. doi: 10.1126/science.1163886

Bradstock RA (2010) A biogeographic model of fire regimes in Australia: current and future implications. Glob Ecol Biogeogr 19:145–158. doi: 10.1111/j.1466-8238.2009.00512.x

Byram GM, Jemison GM (1943) Solar radiation and forest fuel moisture. J Agric Res 67:149–176.

Castillo Soto ME (2012) The identification and assessment of areas at risk of forest fire using fuzzy methodology. Appl Geogr 35:199–207. doi: 10.1016/j.apgeog.2012.07.001

Chakravarti AK (1968) Summer rainfall in India: A review of monsoonal and extramonsoonal aspects –. Atmosphere (Basel) 6:21–28. doi: 10.1080/00046973.1968.9676546

Chand KTR, Badarinath KVS, Murthy MSR, et al. (2007) Active forest fire monitoring in Uttaranchal State, India using multi-temporal DMSP-OLS and MODIS data. Int J Remote Sens 28:2123–2132. doi: 10.1080/01431160600810609

Chen F, Niu S, Tong X, et al. (2014) The impact of precipitation regimes on forest fires in Yunnan Province, Southwest China. Sci World J. doi: 10.1155/2014/326782

Christophe B, Marque J, Foulon B (2010) In-orbit data verification of the accelerometers of the ESA GOCE mission. Socete Fr d’Astronomie d’astrophysique 2–5.

Cochrane MA (2003) Fire science for rainforests. Nature 421:913–919. doi: 10.1038/nature01437

Conedera M, Krebs P, Valese E, et al. (2018) Characterizing Alpine pyrogeography from fire statistics. Appl Geogr 98:87–99. doi: 10.1016/j.apgeog.2018.07.011

Cressie N (1992) STATISTICS FOR SPATIAL DATA. Terra Nov. doi: 10.1111/j.1365-3121.1992.tb00605.x

Cyr D, Gauthier S, Bergeron Y (2007) Scale-dependent determinants of heterogeneity in fire frequency in a coniferous boreal forest of eastern Canada. Landsc Ecol 22:1325–1339. doi: 10.1007/s10980-007-9109-3

de Araújo FM, Ferreira LG, Arantes AE (2012) Distribution Patterns of Burned Areas in the Brazilian Biomes: An Analysis Based on Satellite Data for the 2002-2010 Period. Remote Sens. doi: 10.3390/rs4071929

Deumlich D, Kiesel J, Thiere J, et al. (2006) Application of the SIte COmparison Method (SICOM) to assess the potential erosion risk - a basis for the evaluation of spatial equivalence of agri-environmental measures. Catena 68:141–152. doi: 10.1016/j.catena.2006.04.003

Dimri AP, Chevuturi A (2016) Western Disturbances - An Indian Meteorological Perspective. doi: 10.1007/978-3-319-26737-1

Erten E, Kurgun V, Musao N (1996) Forest Fire Risk Zone Mapping From Satellite. XXth Int Soc Photogramm Remote Sens Congr 4:1–10. doi: 10.1016/S0303-2434(02)00006-5

Fanin T, van der Werf GR (2015) Relationships between burned area, forest cover loss, and land cover change in the Brazilian Amazon based on satellite data. Biogeosciences 12:6033–6043.

doi: 10.5194/bg-12-6033-2015

Fanin T, Van Der Werf GR (2015) Relationships between burned area, forest cover loss, and land cover change in the Brazilian Amazon based on satellite data. Biogeosciences. doi: 10.5194/bg-12-6033-2015

Fares S, Bajocco S, Salvati L, et al. (2017) Characterizing potential wildland fire fuel in live vegetation in the Mediterranean region. Ann For Sci. doi: 10.1007/s13595-016-0599-5

Ferreira JG (2000) Development of an estuarine quality index based on key physical and biogeochemical features. Ocean Coast Manag 43:99–122. doi: 10.1016/S0964-5691(99)00065-4

Flannigan M., Stocks B., Wotton B. (2000) Climate change and forest fires. Sci Total Environ 262:221–229. doi: 10.1016/S0048-9697(00)00524-6

Flannigan M, Cantin AS, De Groot WJ, et al. (2013) Global wildland fire season severity in the 21st century. For Ecol Manage 294:54–61. doi: 10.1016/j.foreco.2012.10.022

Flynn LP, Mouginis-Mark PJ (1995) A comparison of the thermal characteristics of active lava flows and forest fires. Geophys Res Lett 22:2577–2580. doi: 10.1029/95GL02427

Fox DM, Martin N, Carrega P, et al. (2015) Increases in fire risk due to warmer summer temperatures and wildland urban interface changes do not necessarily lead to more fires. Appl Geogr 56:1–12. doi: 10.1016/j.apgeog.2014.10.001

Ganteaume A, Camia A, Jappiot M, et al. (2013) A Review of the Main Driving Factors of Forest Fire Ignition Over Europe. Environ Manage 51:651–662. doi: 10.1007/s00267-012-9961-z

Ganteaume A, Long-Fournel M (2015) Driving factors of fire density can spatially vary at the local scale in south-eastern France. Int J Wildl Fire 24:650–664. doi: 10.1071/WF13209

Getis A, Griffith DA (2002) Comparative Spatial Filtering in Regression Analysis. Geogr Anal 34:130–140. doi: 10.1111/j.1538-4632.2002.tb01080.x

Giglio L, van der Werf GR, Randerson JT, et al. (2006) Global estimation of burned area using MODIS active fire observations. Atmos Chem Phys 6:957–974. doi: 10.5194/acp-6-957-2006

Gillett NP, Weaver AJ, Zwiers FW, Flannigan MD (2004) Detecting the effect of climate change on Canadian forest fires. Geophys Res Lett. doi: 10.1029/2004GL020876

Graeme D. Hutcheson (1999) Ordinary Least-Squares Regression. Multivar. Soc. Sci. SAGE Publications, Ltd., 6 Bonhill Street, London EC2A 4PU, pp 56–113

Habib G, Venkataraman C, Chiapello I, et al. (2006) Seasonal and interannual variability in absorbing aerosols over India derived from TOMS: Relationship to regional meteorology and emissions. Atmos Environ 40:1909–1921. doi: 10.1016/j.atmosenv.2005.07.077

Hernandez C, Drobinski P, Turquety S (2015) How much does weather control fire size and intensity in the Mediterranean region? Ann Geophys 33:931–939. doi: 10.5194/angeo-33-931-2015

IANS (2016) Fire destroys several hectares of forests in Uttar Pradesh. The Hindu 1.

Jaiswal RK, Mukherjee S, Raju KD, Saxena R (2002) Forest fire risk zone mapping from satellite imagery and GIS. Int J Appl Earth Obs Geoinf 4:1–10. doi: 10.1016/S0303-2434(02)00006-5

Joseph S, Anitha K, Murthy MSR (2009) Forest fire in India: a review of the knowledge base. J For Res

14:127–134. doi: 10.1007/s10310-009-0116-x

Jupp TE, Taylor CM, Balzter H, George CT (2006) A statistical model linking Siberian forest fire scars with early summer rainfall anomalies. Geophys Res Lett 33:L14701. doi: 10.1029/2006GL026679

Kahiu MN, Hanan NP (2018) Fire in sub-Saharan Africa: The fuel, cure and connectivity hypothesis. Glob Ecol Biogeogr. doi: 10.1111/geb.12753

Kanevski M, Pereira MG (2017) Local fractality: The case of forest fires in Portugal. Phys A Stat Mech its Appl 479:400–410. doi: 10.1016/j.physa.2017.02.086

Kiran Chand TR, Badarinath KVS, Krishna Prasad V, et al. (2006) Monitoring forest fires over the Indian region using Defense Meteorological Satellite Program-Operational Linescan System nighttime satellite data. Remote Sens Environ 103:165–178. doi: 10.1016/j.rse.2006.03.010

Kirkpatrick JB, Marsden-Smedley JB, Leonard SWJ (2011) Influence of grazing and vegetation type on post-fire flammability. J Appl Ecol 48:642–649. doi: 10.1111/j.1365-2664.2011.01962.x

KODANDAPANI N, COCHRANE MA, SUKUMAR R (2004) Conservation Threat of Increasing Fire Frequencies in the Western Ghats, India. Conserv Biol 18:1553–1561. doi: 10.1111/j.1523-1739.2004.00433.x

Krawchuk MA, Cumming SG, Flannigan MD, Wein RW (2006) BIOTIC AND ABIOTIC REGULATION OF LIGHTNING FIRE INITIATION IN THE MIXEDWOOD BOREAL FOREST. Ecology 87:458–468. doi: 10.1890/05-1021

Krider EP, Noggle RC, Pifer AE, Vance DL (1980) Lightning Direction-Finding Systems for Forest Fire Detection. Bull Am Meteorol Soc 61:980–986. doi: 10.1175/1520-0477(1980)061<0980:LDFSFF>2.0.CO;2

Kumar N, Yadav BP, Gahlot S, Singh M (2015) Winter frequency of western disturbances and precipitation indices over Himachal Pradesh, India: 1977-2007. Atmósfera 28:63–70. doi: 10.1016/S0187-6236(15)72160-0

Lasaponara R, Simoniello T, Masini N, Cuomo V (2004) Performance evaluation of AVHRR-based methods for the estimation of fire susceptibility in southern Italy. In: Owe M, D’Urso G, Moreno JF, Calera A (eds)p 219

Laurance WF, Albernaz AKM, Costa C Da (2001) Is deforestation accelerating in the Brazilian Amazon? Environ Conserv. doi: 10.1017/S0376892901000339

Laurent P, Mouillot F, Yue C, et al. (2018) FRY, a global database of fire patch functional traits derived from space-borne burned area products. Sci Data 5:180132. doi: 10.1038/sdata.2018.132

Liu Z, Wimberly MC (2016) Direct and indirect effects of climate change on projected future fire regimes in the western United States. Sci Total Environ 542:65–75. doi: 10.1016/j.scitotenv.2015.10.093

Mancini LD, Corona P, Salvati L (2018) Ranking the importance of Wildfires’ human drivers through a multi-model regression approach. Environ Impact Assess Rev 72:177–186. doi: 10.1016/j.eiar.2018.06.003

Mann ML, Batllori E, Moritz MA, et al. (2016) Incorporating Anthropogenic Influences into Fire

Probability Models: Effects of Human Activity and Climate Change on Fire Activity in California. PLoS One 11:e0153589. doi: 10.1371/journal.pone.0153589

McKinney W, Team PD (2015) Pandas - Powerful Python Data Analysis Toolkit. Pandas - Powerful Python Data Anal Toolkit 1625.

Meng Q, Meentemeyer RK (2011) Modeling of multi-strata forest fire severity using Landsat TM Data. Int J Appl Earth Obs Geoinf 13:120–126. doi: 10.1016/j.jag.2010.08.002

Microsoft® (2016) Trendline Analysis in Excel 2016. 1–5.

Mooley DA (1957) The role of western disturbances in the production of weather over India during different seasons. Indian J Meteor Geophys 8:253–260.

Murthy CS, Singh J, Kumar P, Sesha Sai MVR (2016) Meteorological drought analysis over India using analytical framework on CPC rainfall time series. Nat Hazards 81:573–587. doi: 10.1007/s11069-015-2097-8

Nepstad DC, Stickler CM, Filho BS, Merry F (2008) Interactions among Amazon land use, forests and climate: prospects for a near-term forest tipping point. Philos Trans R Soc B Biol Sci 363:1737–1746. doi: 10.1098/rstb.2007.0036

Nogueira J, Rambal S, Barbosa J, Mouillot F (2017) Spatial Pattern of the Seasonal Drought/Burned Area Relationship across Brazilian Biomes: Sensitivity to Drought Metrics and Global Remote-Sensing Fire Products. Climate 5:42. doi: 10.3390/cli5020042

Nunes MCS, Vasconcelos MJ, Pereira JMC, et al. (2005) Land Cover Type and Fire in Portugal: Do Fires Burn Land Cover Selectively? Landsc Ecol 20:661–673. doi: 10.1007/s10980-005-0070-8

Paniello RC, Neely JG, Rich JT, et al. (2011) Practical guide to choosing an appropriate data display. Otolaryngol - Head Neck Surg 145:886–894. doi: 10.1177/0194599811423608

Pechony O, Shindell DT (2010) Driving forces of global wildfires over the past millennium and the forthcoming century. Proc Natl Acad Sci 107:19167–19170. doi: 10.1073/pnas.1003669107

Pinchot G (2011) The Relation of Forests and Forest Fires by Gifford Pinchot, with an Introduction by James K. Agee. Fire Ecol 7:2–11. doi: 10.4996/fireecology.0703002

Prasad VK, Badarinath KVS, Eaturu A (2008) Biophysical and anthropogenic controls of forest fires in the Deccan Plateau, India. J Environ Manage 86:1–13. doi: 10.1016/j.jenvman.2006.11.017

Ravindranath NH, Somashekhar BS, Gadgil M (1997) Carbon flow in Indian forests. Clim Change. doi: 10.1023/A:1005303405404

Read N, Duff TJ, Taylor PG (2018) A lightning-caused wildfire ignition forecasting model for operational use. Agric For Meteorol 253–254:233–246. doi: 10.1016/j.agrformet.2018.01.037

Renkin RA, Despain DG (1992) Fuel moisture, forest type, and lightning-caused fire in Yellowstone National Park. Can J For Res 22:37–45. doi: 10.1139/x92-005

Robert H. Shumway and David S. Stoffer (2006) Time Series Regression and Exploratory Data Analysis. Time Ser. Anal. Its Appl. Springer New York, pp 48–83

Ruosteenoja K, Räisänen P (2013) Seasonal Changes in Solar Radiation and Relative Humidity in Europe in Response to Global Warming*. J Clim 26:2467–2481. doi: 10.1175/JCLI-D-12-00007.1

Said Guettouche M, Derias A (2013) Modelling of Environment Vulnerability to Forests Fires and Assessment by GIS Application on the Forests of Djelfa (Algeria). J Geogr Inf Syst 05:24–32. doi: 10.4236/jgis.2013.51003

Stocks BJ, Mason JA, Todd JB, et al. (2002) Large forest fires in Canada, 1959–1997. J Geophys Res 108:8149. doi: 10.1029/2001JD000484

Sujatha ER, Rajamanickam GV (2015) Landslide Hazard and Risk Mapping Using the Weighted Linear Combination Model Applied to the Tevankarai Stream Watershed, Kodaikkanal, India. Hum Ecol Risk Assess 21:1445–1461. doi: 10.1080/10807039.2014.920222

Swartman RK, Ogunlade O (1967) A statistical relationship between solar radiation,' sunshine and relative humidity in the tropics. Atmosphere (Basel) 5:25–34. doi: 10.1080/00046973.1967.9676534

Tansey K, Grégoire J-M, Defourny P, et al. (2008) A new, global, multi-annual (2000–2007) burnt area product at 1 km resolution. Geophys Res Lett 35:L01401. doi: 10.1029/2007GL031567

Thackway R, Mutendeudzi M, Kelley G (2008) Assessing the extent of Australia's forest burnt by planned and unplanned fire. 30.

Uhl C, Kauffman JB (2012) Deforestation , Fire Susceptibility , and Potential Tree Responses to Fire in the Eastern Amazon Author (s): Christopher Uhl and J . Boone Kauffman Reviewed work (s): Published by : Ecological Society of America Stable URL : http://www.jstor.org/stabl. Ecology 71:437–449.

Van Der Werf GR, Randerson JT, Giglio L, et al. (2008) Climate controls on the variability of fires in the tropics and subtropics. Global Biogeochem Cycles 22:1–13. doi: 10.1029/2007GB003122

Westerling AL (2006) Warming and Earlier Spring Increase Western U.S. Forest Wildfire Activity. Science (80-) 313:940–943. doi: 10.1126/science.1128834

Westerling ALR (2016) Increasing western US forest wildfire activity: Sensitivity to changes in the timing of spring. Philos Trans R Soc B Biol Sci. doi: 10.1098/rstb.2015.0178

Xie P, Chen M, Shi W (2010) CPC unified gauge-based analysis of global daily precipitation. Prepr. 24th Conf. Hydrol. Atlanta, GA, Amer. Meteor. Soc 2:

You W, Lin L, Wu L, et al. (2017) Geographical information system-based forest fire risk assessment integrating national forest inventory data and analysis of its spatiotemporal variability. Ecol Indic 77:176–184. doi: 10.1016/j.ecolind.2017.01.042

List of figures

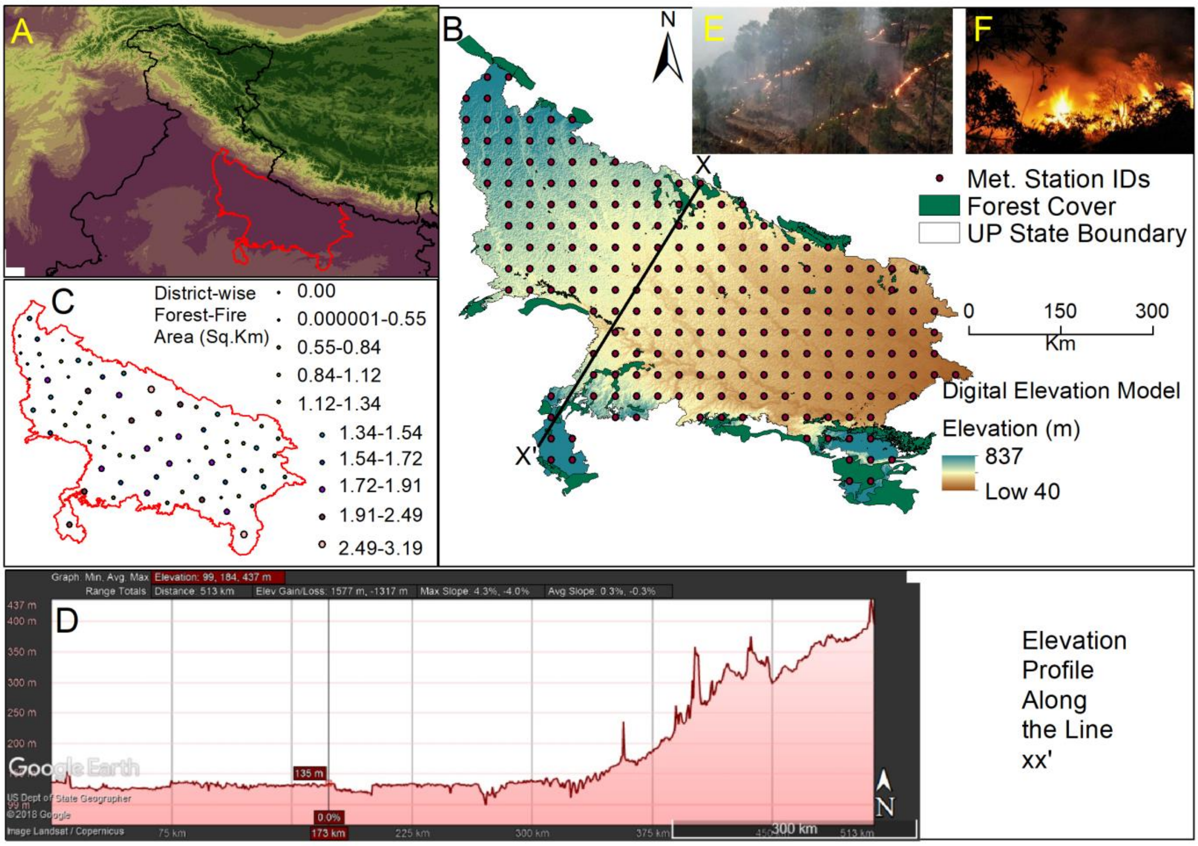

Figure (1): Location Map of the study area. A. location of Uttar Pradesh, marked with red colour, on the map of India showing international boundaries is shown. B. in Uttar Pradesh sites of meteorological station IDs is presented. Part C displays District wise forest coverage in Uttar Pradesh. In Part D of the figure, Google Earth Pro derived elevation profile; along the line X’X is shown. E and F are photos of the fire events in different parts of the study area.

```
import glob, os
import pandas as pd
os.chdir('E:\Work\New_Papers\UP Forest Fire\CFSR Weather Data\UP\UP1')
results = pd.DataFrame([])
for counter, file in enumerate(glob.glob("weatherdata*")):
    namedf = pd.read_csv(file, skiprows=0, usecols=[1,2,3])
    results = results.append(namedf)

results.to_csv('E:\Work\New_Papers\UP Forest Fire\CFSR Weather Data\UP\UP1\combinedfile1.csv')
```

Figure (2): Python Script for CFSR Data Extraction

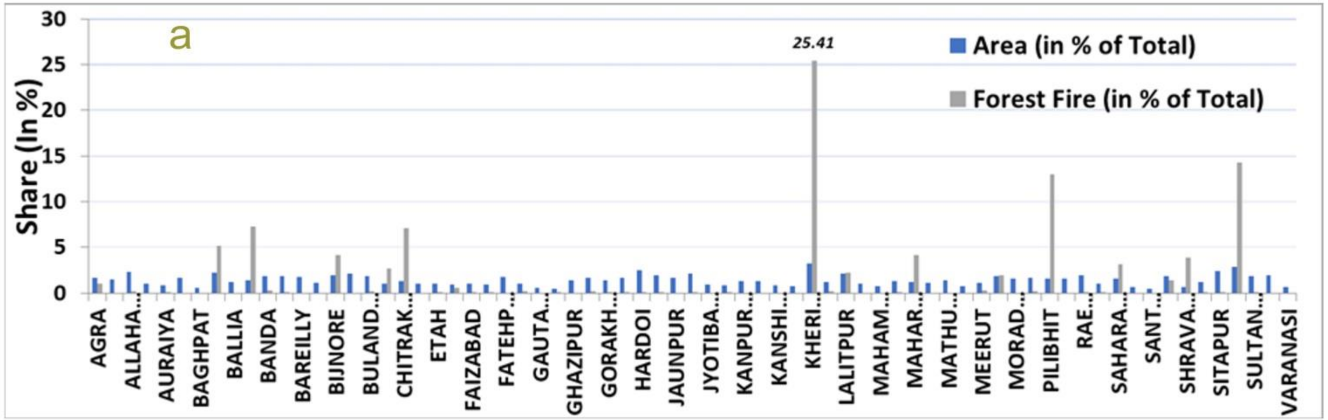

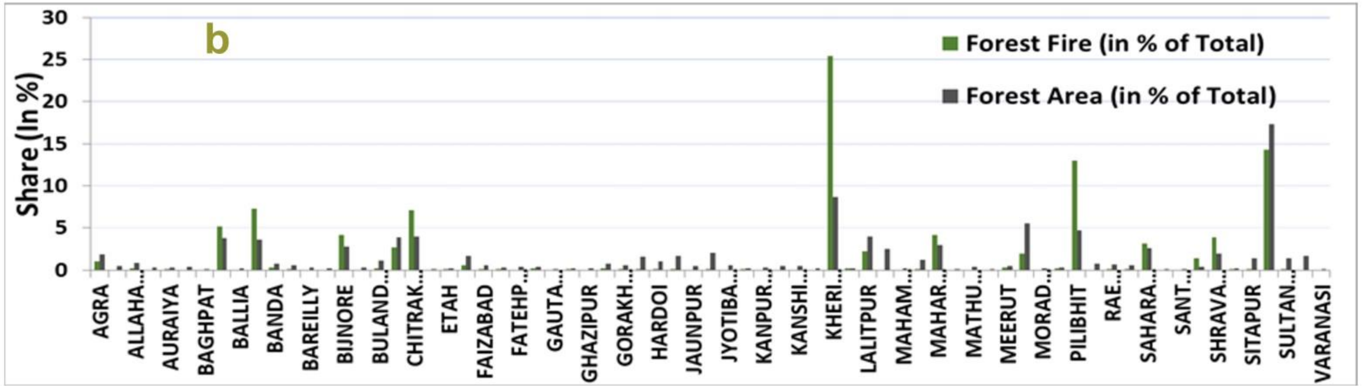

Figure (3a): District wise "total district area (forested and non-forested both) versus forest fire" distribution of Uttar Pradesh. (3b): District wise total forest-cover (forested area only) and forest fire distribution of Uttar Pradesh

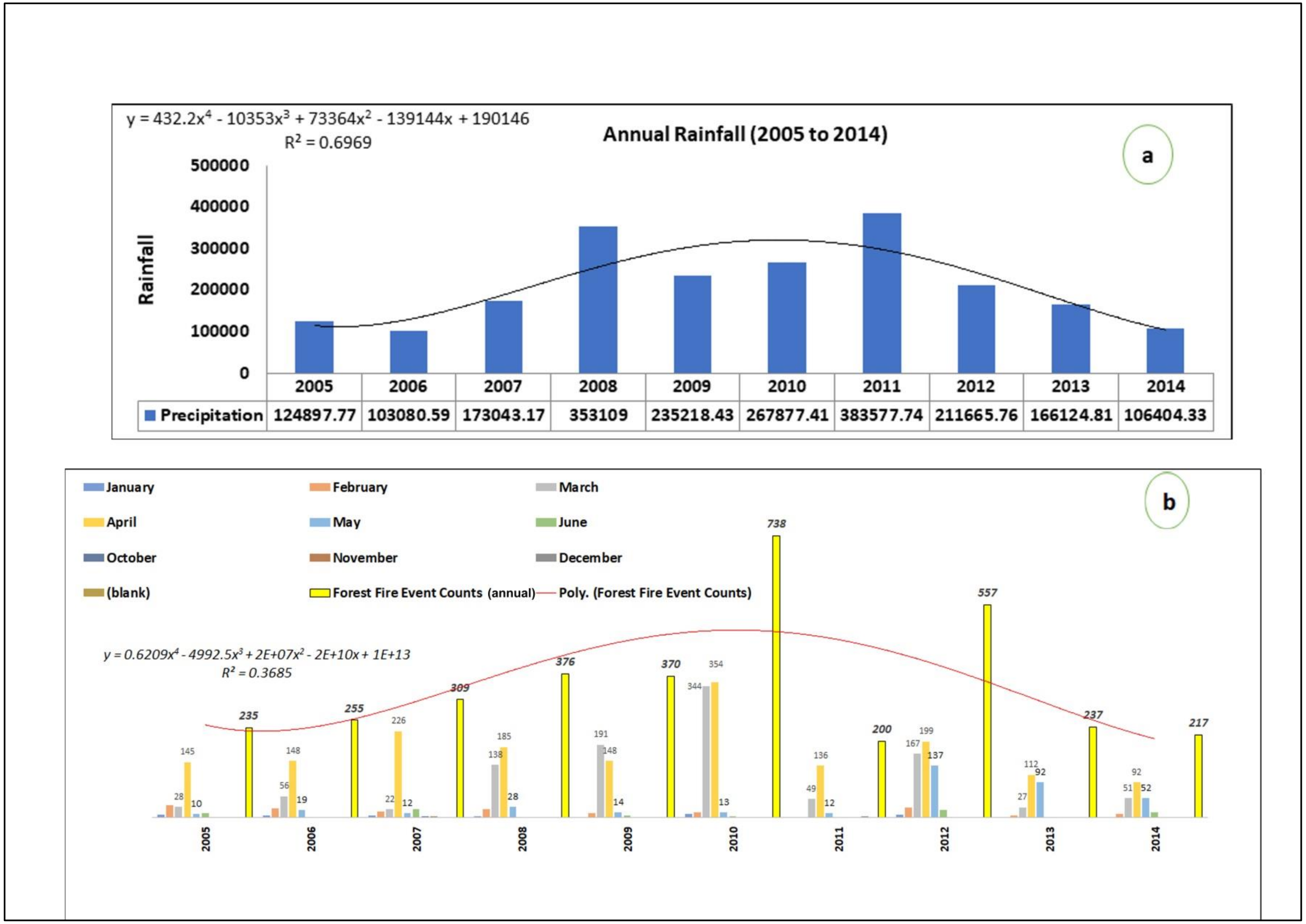

Figure (4) a: Annual rainfall over the period 2005-2014. b: monthly and annual forest fire count data presented a trend similar to the rainfall data both of which are fitted at 4th order polynomial function. The similarity of trend in both of these parameters (annual precipitation trend shown by black line in the upper graph and annual forest fire trend by red line in the lower graph) is considered to be indicator of underlying functional linkage.

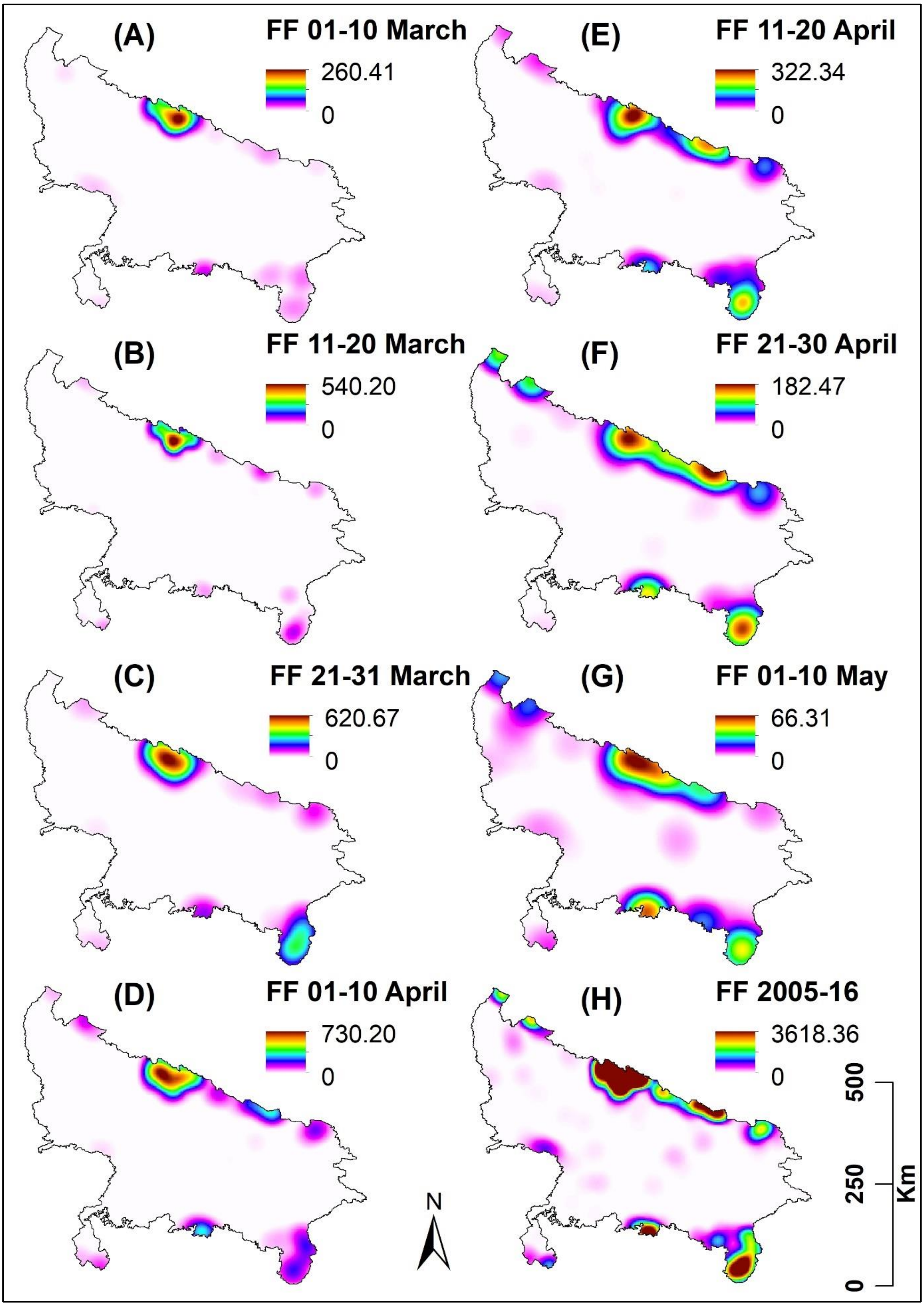

Figure (5): Forest Fire Count (FFC) data interpolated using IDW method to see the spatial trend in the changing behavior of fire events at 10-day interval during the study period. The 7 map sections (A to H) show how areas of higher FFCs have shifted from Cluster B to Cluster E. (for location of clusters, refer to supplementary figure 2). Map H shows distribution of total FFCs over the 11 year study period in the area and indicates the clustering of FFCs mainly in Clusters B and E.

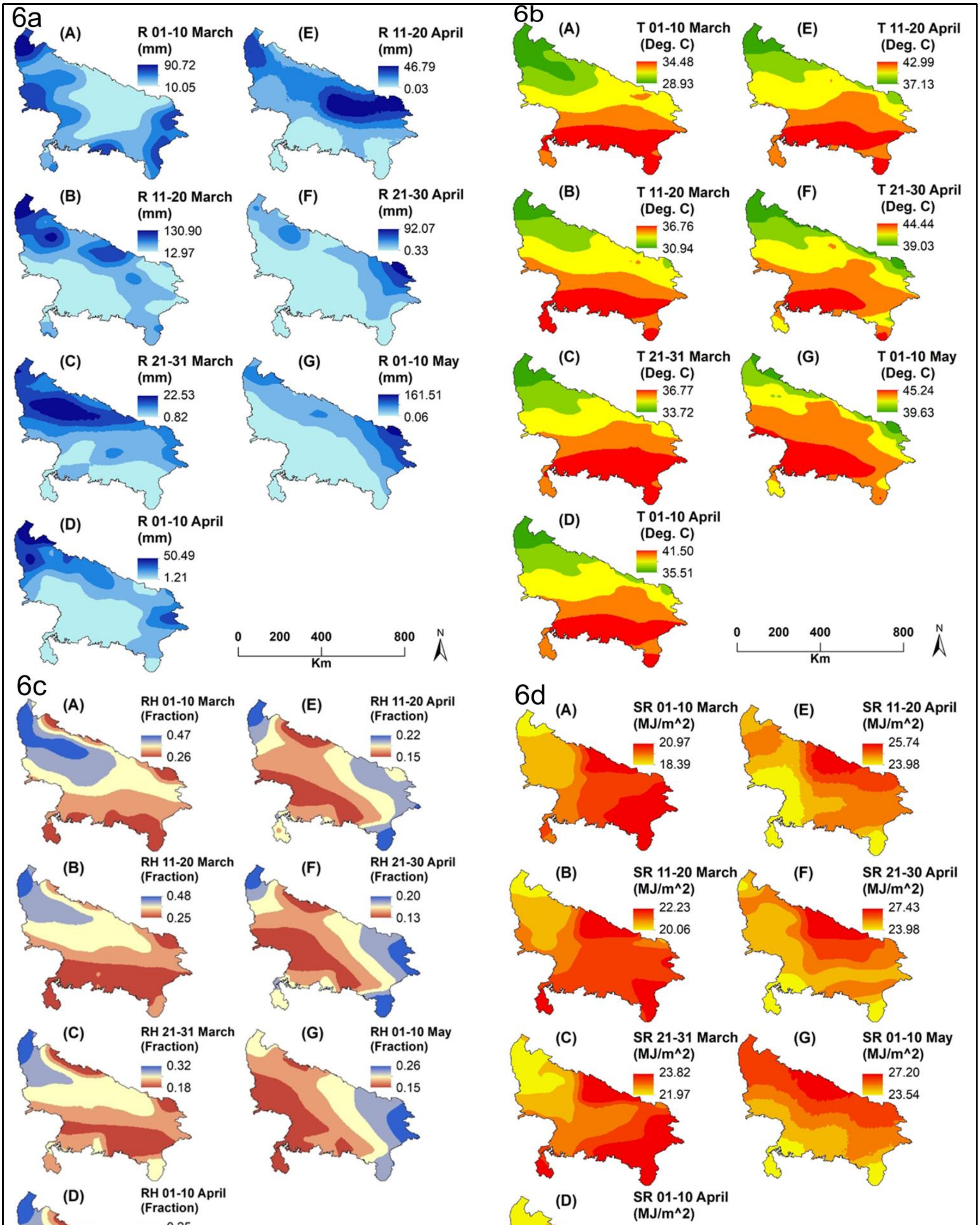
6a
(A)
R 01-10 March (mm)
90.72
10.05
(E)
R 11-20 April (mm)
46.79
0.03
(B)
R 11-20 March (mm)
130.90
12.97
(F)
R 21-30 April (mm)
92.07
0.33
(C)
R 21-31 March (mm)
22.53
0.82
(G)
R 01-10 May (mm)
161.51
0.06
(D)
R 01-10 April (mm)
50.49
1.21
0 200 400 800
Km
N
6b
(A)
T 01-10 March (Deg. C)
34.48
28.93
(E)
T 11-20 April (Deg. C)
42.99
37.13
(B)
T 11-20 March (Deg. C)
36.76
30.94
(F)
T 21-30 April (Deg. C)
44.44
39.03
(C)
T 21-31 March (Deg. C)
36.77
33.72
(G)
T 01-10 May (Deg. C)
45.24
39.63
(D)
T 01-10 April (Deg. C)
41.50
35.51
0 200 400 800
Km
N
6c
(A)
RH 01-10 March (Fraction)
0.47
0.26
(E)
RH 11-20 April (Fraction)
0.22
0.15
(B)
RH 11-20 March (Fraction)
0.48
0.25
(F)
RH 21-30 April (Fraction)
0.20
0.13
(C)
RH 21-31 March (Fraction)
0.32
0.18
(G)
RH 01-10 May (Fraction)
0.26
0.15
(D)
RH 01-10 April (Fraction)
0.25
0.16
0 200 400 800
Km
N
6d
(A)
SR 01-10 March (MJ/m^2)
20.97
18.39
(E)
SR 11-20 April (MJ/m^2)
25.74
23.98
(B)
SR 11-20 March (MJ/m^2)
22.23
20.06
(F)
SR 21-30 April (MJ/m^2)
27.43
23.98
(C)
SR 21-31 March (MJ/m^2)
23.82
21.97
(G)
SR 01-10 May (MJ/m^2)
27.20
23.54
(D)
SR 01-10 April (MJ/m^2)
25.21
23.09
0 200 400 800
Km
N

Figure (6): Rainfall (R) (figure 6a), Temperature (T) (figure 6b), Relative Humidity (RH) (figure 6c), and Solar radiation (SR) (figure 6d) data have been mapped with IDW interpolation method to see the spatial trend in the changing behavior of these meteorological variables *vis-à-vis* fire events at 10-day interval during the study period. The 7 map sections (A to G) show variability of the variables in different clusters (for location of clusters, refer to supplementary figure 2).

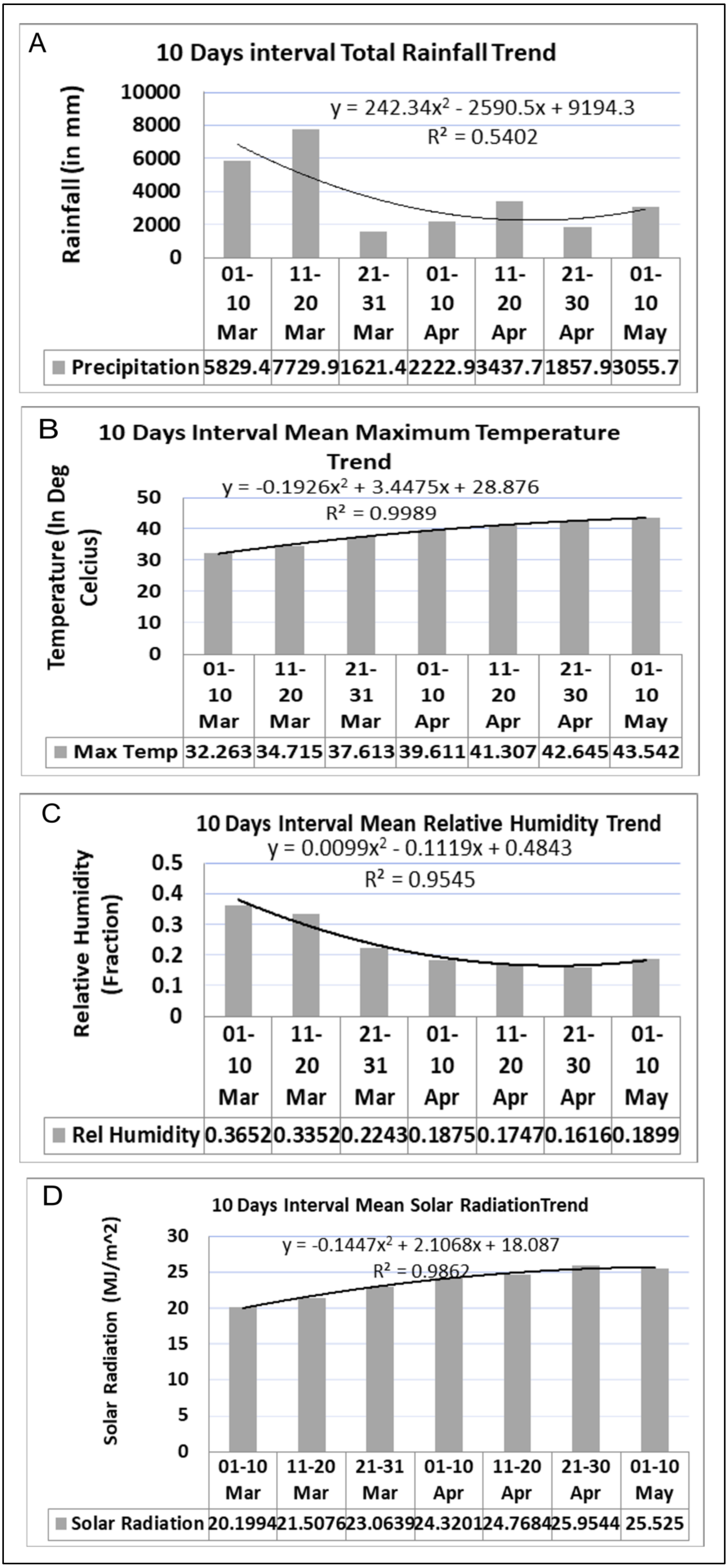
A
10 Days interval Total Rainfall Trend
Rainfall (in mm)
10000
8000
6000
4000
2000
0
y = 242.34x² - 2590.5x + 9194.3
R² = 0.5402
01-10 Mar
11-20 Mar
21-31 Mar
01-10 Apr
11-20 Apr
21-30 Apr
01-10 May
Precipitation 5829.4 7729.9 1621.4 2222.9 3437.7 1857.9 3055.7
B
10 Days Interval Mean Maximum Temperature Trend
Temperature (In Deg Celcius)
50
40
30
20
10
0
y = -0.1926x² + 3.4475x + 28.876
R² = 0.9989
01-10 Mar
11-20 Mar
21-31 Mar
01-10 Apr
11-20 Apr
21-30 Apr
01-10 May
Max Temp 32.263 34.715 37.613 39.611 41.307 42.645 43.542
C
10 Days Interval Mean Relative Humidity Trend
Relative Humidity (Fraction)
0.5
0.4
0.3
0.2
0.1
0
y = 0.0099x² - 0.1119x + 0.4843
R² = 0.9545
01-10 Mar
11-20 Mar
21-31 Mar
01-10 Apr
11-20 Apr
21-30 Apr
01-10 May
Rel Humidity 0.3652 0.3352 0.2243 0.1875 0.1747 0.1616 0.1899
D
10 Days Interval Mean Solar RadiationTrend
Solar Radiation (MJ/m^2)
30
25
20
15
10
5
0
y = -0.1447x² + 2.1068x + 18.087
R² = 0.9862
01-10 Mar
11-20 Mar
21-31 Mar
01-10 Apr
11-20 Apr
21-30 Apr
01-10 May
Solar Radiation 20.1994 21.5076 23.0639 24.3201 24.7684 25.9544 25.525

Figure (7): Trend in the rainfall (A), in mean maximum temperature (B), mean relative humidity (C), and Solar radiation (D) at 10-days interval over the entire study period. During the entire 11 year of study period, the rainfall has been observed to first decrease from March to May. The late March rainfall in the study area is influenced by western disturbances (WDs; Chakravarti 1968, Dimri & Chevuturi 2016, Kumar *et al.* 2015, Mooley 1957) which diminishes as the summer season advances. Temperature trend shows gradual increasing T values which are helpful in conditions favouring risk of forest fire ignition trigger as well as fire expansion whereas mean relative humidity and solar radiation show decreasing and increasing trend over the study period, respectively.

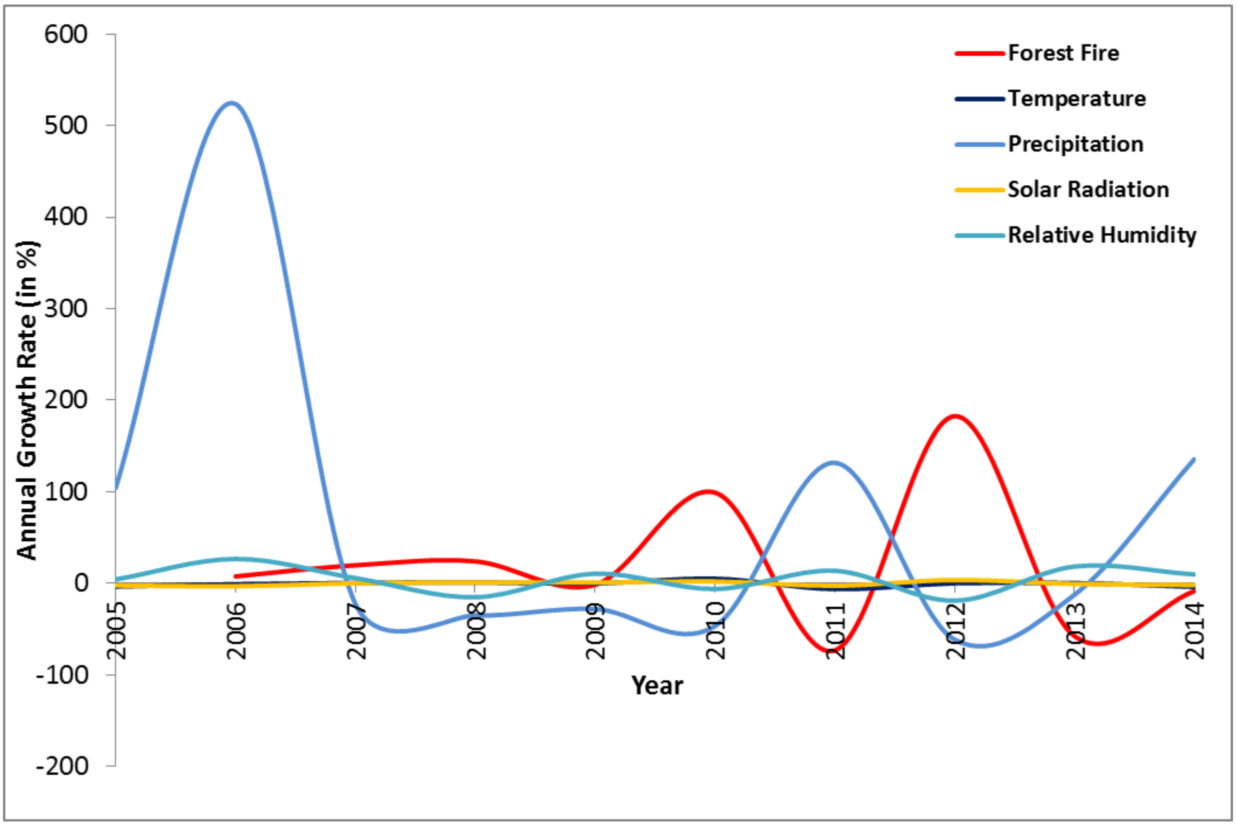

Figure (8): Increment Rate (defined in the methodology section) showing trend in different meteorological variables vis-à-vis forest fire events. This graph clearly shows the how forest fires are positively or negatively interrelated to rainfall (precipitation in the index in this graph) and relative humidity. Relation between forest fire IRs and those of solar radiation and temperature are not very clear.

List of tables

Table (1): Parameters used to project the vector layers of FFC and meteorological vector datasets in order to compute spatial distribution over the study area

Parameter	Projection	Spheroid	Datum	UTM Zone
Fire data points	Universal Transverse Mercator (UTM) Projection System	WGS 84	WGS 84	44N
Met Parameters				

Table (2): Range of FFC and meteorological parameters used for classification and combination matrix construction

CLASS / PARAMETERS	VERY LOW (VL)	LOW (L)	MEDIUM (M)	HIGH (H)	VERY HIGH (VH)
FOREST FIRE COUNT (FFC)	0-150	151-300	301-450	451-600	601-730
RAINFALL (R) IN MM.	0-30	31-60	61-90	91-120	121-161
TEMP (T) IN °C	0-9	10-19	20-29	30-38	38-45
SOLAR RADIATION (SR)	18.39-20.20	20.21-22.02	22.03-23.94	23.95-25.76	25.77-27.42
REL. HUMIDITY (RH) IN FRACTION	0.13-0.19	0.20-0.26	0.27-0.33	0.34-0.41	0.41-0.48

Table (3): Forested area, forest fire count (FFC), forest fire density (FFD) and forest type in each cluster

Clusters	FC (km^2)	Forest Fire Count (FFC)	Forest Fire Density (FFD)	Forest Type
B	48503	2618	5.397604	Tropical Dry Deciduous, Tropical Moist Deciduous
E	20694	1139	5.504011	Tropical Dry Deciduous
D	17772	104	0.58519	Tropical Thorny, Tropical Dry Deciduous, Tropical Moist Deciduous
A	12258	319	2.602382	Sub-Tropical (Coniferous), Himalayan Moist Temperate, Tropical Dry Deciduous, Tropical Moist Deciduous
C	10709	78	0.728359	Tropical Thorny, Tropical Dry

				Deciduous, Tropical Moist Deciduous

Table (4): Comparing ordering of forest coverage (FC) and forest fire density (FFD)

←Increasing order of magnitude towards left←					
Variable	Cluster Code				
FC	B (48503 km2)<	E (20694 km2)<	D (17772 km2)<	A (12258 km2)<	C (10709 km2)
FFD	B (5.40)<	E (5.50)<	A (0.56)<	C (2.60)<	D (0.73)

Table (5): Percentage share of FFC events of different categories

Parameter Code	Class Code				
FFC / Code	VL	L	M	H	VH
% Share	60	22.85714	5.714286	5.714286	5.714286

Table (6): Combination Matrix Illustrating Combinations of Meteorological Parameter Classes for Different Classes of Forest Fire Count (FFC)

TIME-CLUSTER ZONE	CLASS	VERY LOW (VL)	LOW (L)	MEDIUM (M)	HIGH (H)	VERY HIGH (VH)
1-10 March	**CLUSTER-A**	$VL_{FFC} \rightarrow \{ H_{R}-M_{T}-VH_{RH}-VL_{SR} \}$				
	CLUSTER-B		$L_{FFC} \rightarrow \{ VL_{R}-H_{T}-M_{RH}-L_{SR} \}$			
	CLUSTER-C	$VL_{FFC} \rightarrow \{ M_{R}-H_{T}-V_{RH}-VL_{SR} \}$				
	CLUSTER-D	$VL_{FFC} \rightarrow \{ H_{R}-H_{T}-L_{RH}-L_{SR} \}$				
	CLUSTER-E	$VL_{FFC} \rightarrow \{ M_{R}-H_{T}-L_{RH}-L_{SR} \}$				
11-20 March	**CLUSTER-A**	$VL_{FFC} \rightarrow \{ VH_{R}-H_{T}-VH_{RH}-VL_{SR} \}$				
	CLUSTER-B				$H_{FFC} \rightarrow \{ H_{R}-H_{T}-H_{RH}-L_{SR} \}$	
	CLUSTER-C	$VL_{FFC} \rightarrow \{ VL_{R}-H_{T}-H_{RH}-L_{SR} \}$				
	CLUSTER-D	$VL_{FFC} \rightarrow \{ H_{R}-H_{T}-L_{RH}-L_{SR} \}$				
	CLUSTER-E	$VL_{FFC} \rightarrow \{ M_{R}-H_{T}-L_{RH}-M_{SR} \}$				
21-31 March	**CLUSTER-A**	$VL_{FFC} \rightarrow \{ VL_{R}-H_{T}-M_{RH}-L_{SR} \}$				
	CLUSTER-B					$VH_{FFC} \rightarrow \{ VL_{R}-H_{T}-L_{RH}-M_{SR} \}$
	CLUSTER-C		$L_{FFC} \rightarrow \{ VL_{R}-H_{T}-L_{RH}-M_{SR} \}$			
	CLUSTER-D	$VL_{FFC} \rightarrow \{ VL_{R}-H_{T}-L_{RH}-M_{SR} \}$				
	CLUSTER-E			$M_{FFC} \rightarrow \{ VL_{R}-H_{T}-L_{RH}-H_{SR} \}$		
1-10 April	**CLUSTER-A**	$VL_{FFC} \rightarrow \{ L_{R}-H_{T}-L_{RH}-M_{SR} \}$				
	CLUSTER-B					$VH_{FFC} \rightarrow \{ L_{R}-H_{T}-L_{RH}-H_{SR} \}$
	CLUSTER-C		$L_{FFC} \rightarrow \{ VL_{R}-VH_{T}-L_{RH}-M_{SR} \}$			
	CLUSTER-D	$VL_{FFC} \rightarrow \{ VL_{R}-VH_{T}-L_{RH}-H_{SR} \}$				
	CLUSTER-E				$H_{FFC} \rightarrow \{ VL_{R}-VH_{T}-L_{RH}-H_{SR} \}$	
11-20 April	**CLUSTER-A**	$VL_{FFC} \rightarrow \{ L_{R}-H_{T}-L_{RH}-M_{SR} \}$				
	CLUSTER-B			$M_{FFC} \rightarrow \{L_{R}-VH_{T}-H_{RH}-VL_{SR}\}$		
	CLUSTER-C		$L_{FFC} \rightarrow \{ VL_{R}-VH_{T}-VL_{RH}-H_{SR} \}$			
	CLUSTER-D	$VL_{FFC} \rightarrow \{ VL_{R}-VH_{T}-VL_{RH}-H_{SR} \}$				
	CLUSTER-E		$L_{FFC} \rightarrow \{ VL_{R}-VH_{T}-L_{RH}-H_{SR} \}$			
21-30 April	**CLUSTER-A**		$L_{FFC} \rightarrow \{ M_{R}-VH_{T}-L_{RH}-H_{SR} \}$			
	CLUSTER-B		$L_{FFC} \rightarrow \{ M_{R}-VH_{T}-L_{RH}-VH_{SR} \}$			
	CLUSTER-C	$VL_{FFC} \rightarrow \{ VL_{R}-VH_{T}-VL_{RH}-H_{SR} \}$				
	CLUSTER-D	$VL_{FFC} \rightarrow \{ VL_{R}-VH_{T}-VL_{RH}-H_{SR} \}$				
	CLUSTER-E		$L_{FFC} \rightarrow \{ VL_{R}-VH_{T}-L_{RH}-H_{SR} \}$			
1-10 May	**CLUSTER-A**	$VL_{FFC} \rightarrow \{ H_{R}-VH_{T}-L_{RH}-VH_{SR} \}$				
	CLUSTER-B	$VL_{FFC} \rightarrow \{ H_{R}-VH_{T}-VL_{RH}-VH_{SR} \}$				
	CLUSTER-C	$VL_{FFC} \rightarrow \{ VL_{R}-VH_{T}-VL_{RH}-VH_{SR} \}$				
	CLUSTER-D	$VL_{FFC} \rightarrow \{ VL_{R}-VH_{T}-VL_{RH}-H_{SR} \}$				
	CLUSTER-E	$VL_{FFC} \rightarrow \{ VL_{R}-VH_{T}-L_{RH}-M_{SR} \}$				

Supplementary tables and figures

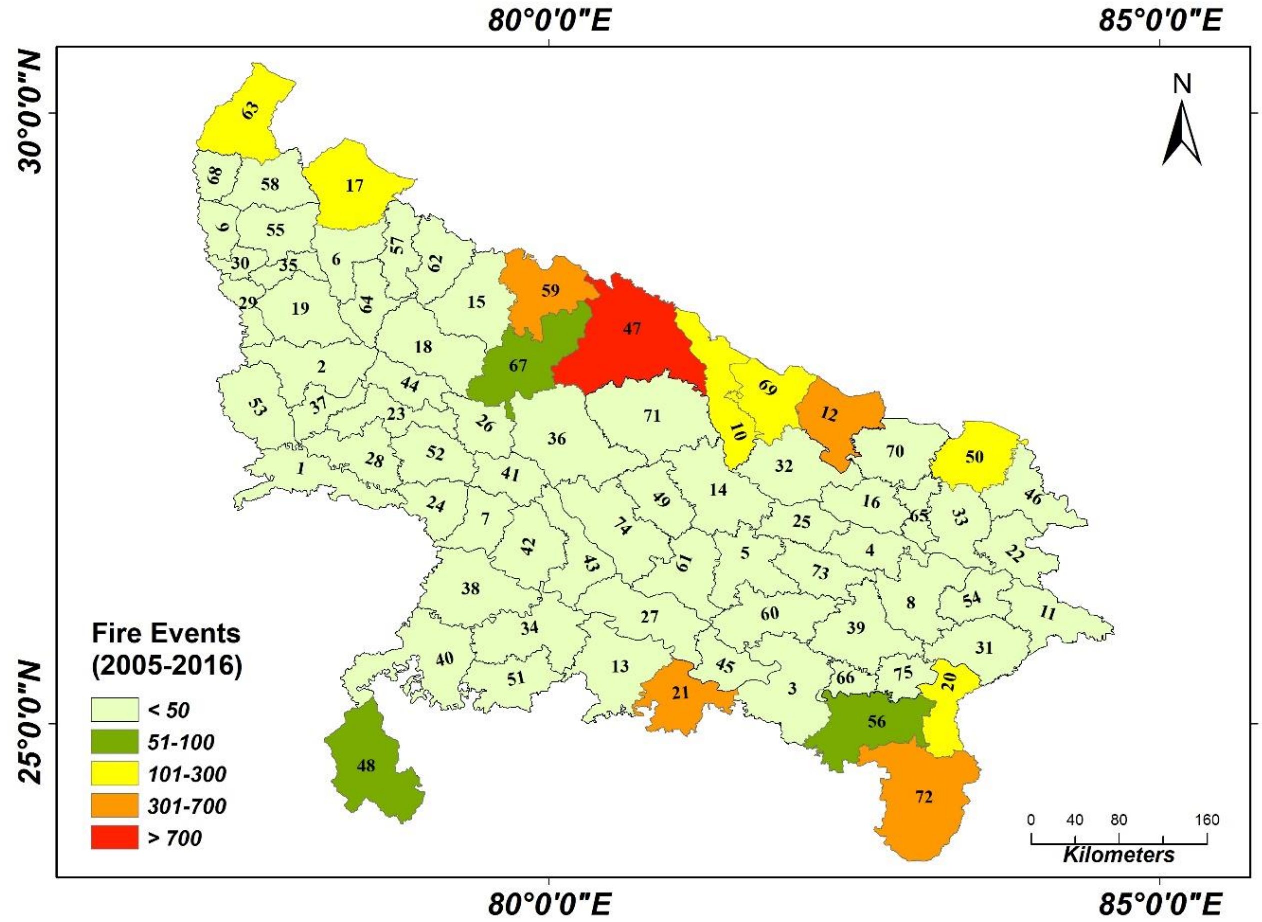

Supplementary Figure (1): District Wise Forest Fire Count data interpolated within district boundaries using IDW kriging method. Numbers in the map show serial number of district names provided in supplementary table number (1). Forest fire counts (FFCs) range has been represented with colour code given in the legend. The digits in front of each colour in the legend represent number of forest fire event counts. The map shows that (with reference to map 2) most of the high FFC events are concentrated in clusters B and E.

Supplementary Table (1): District codes with respective names. The codes are given in the map (supplementary figure 1) showing district wise forest fire counts (FFCs)

Code No	District Name	Code No	District Name	Code No	District Name
1	Agra	26	Farrukhabad	51	Mahoba
2	Aligarh	27	Fatehpur	52	Mainpuri
3	Allahabad	28	Firozabad	53	Mathura
4	Ambedkar Nagar	29	Gautam Buddha Nagar	54	Mau
5	Amethi	30	Ghaziabad	55	Meerut
6	Amroha	31	Ghazipur	56	Mirzapur
7	Auraiya	32	Gonda	57	Moradabad
8	Azamgarh	33	Gorakhpur	58	Muzaffarnagar
9	Baghpat	34	Hamirpur	59	Pilibhit
10	Bahraich	35	Hapur	60	Pratapgarh
11	Ballia	36	Hardoi	61	Rae Bareli
12	Balrampur	37	Hathras	62	Rampur
13	Banda	38	Jalaun	63	Saharanpur
14	Barabanki	39	Jaunpur	64	Sambhal
15	Bareilly	40	Jhansi	65	Sant Kabir Nagar
16	Basti	41	Kannauj	66	Sant Ravi Das Nagar
17	Bijnor	42	Kanpur Dehat	67	Shahjahanpur
18	Budaun	43	Kanpur Nagar	68	Shamli
19	Bulandshahr	44	Kasganj	69	Shravasti
20	Chandauli	45	Kaushambi	70	Siddharth Nagar
21	Chitrakoot	46	Kushinagar	71	Sitapur
22	Deoria	47	Lakhimpur Kheri	72	Sonbhadra
23	Etah	48	Lalitpur	73	Sultanpur
24	Etawah	49	Lucknow	74	Unnao
25	Faizabad	50	Maharajganj	75	Varanasi

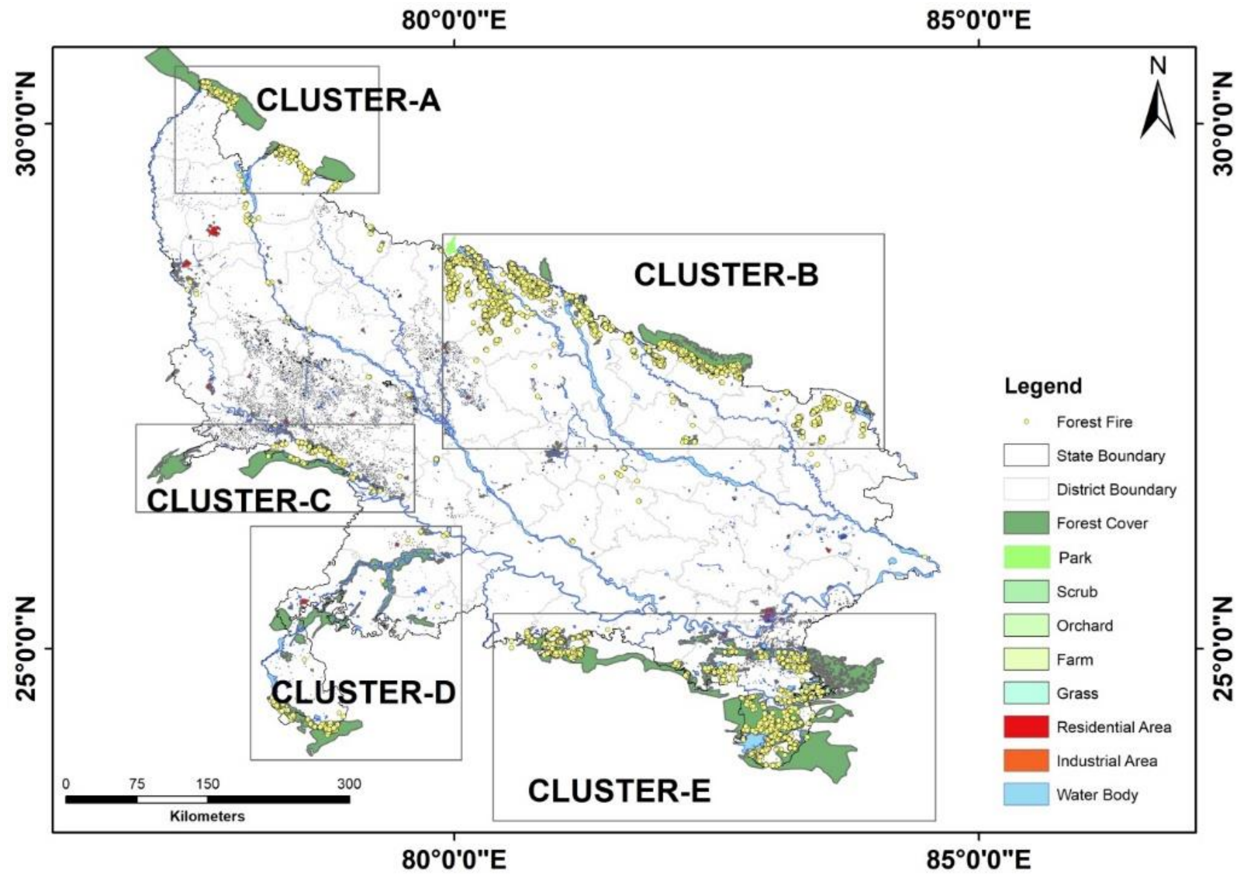

Supplementary Figure (2): Vegetation clusters in different districts of Uttar Pradesh and forest fire events clustered in different parts of the study area

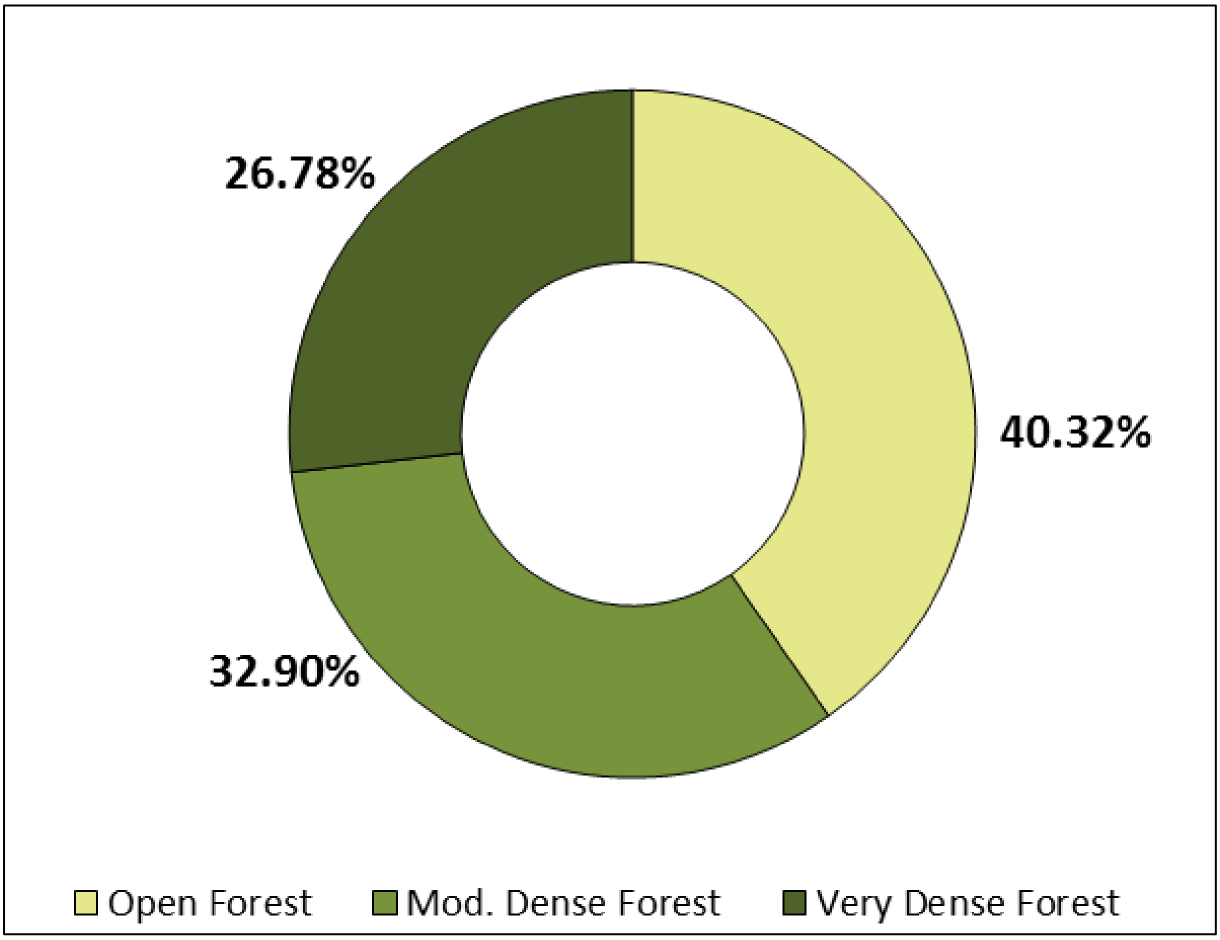

Supplementary Figure (3): Type of forest cover (Source: IFSR, 2017)

Supplementary Table (2): Categorization of Various Parameters into VH, H, M, L, and VL Classes

CLASS / PARAMETERS	VERY LOW (VL)	LOW (L)	MEDIUM (M)	HIGH (H)	VERY HIGH (VH)
FOREST FIRE DENSITY (FFD)	0-150	151-300	301-450	451-600	601-730
RAINFALL (R) IN MM.	0-30	31-60	61-90	91-120	121-161
TEMP (T) IN °C	0-9	10-19	20-29	30-38	38-45
SOLAR RADIATION (SR)	18.39-20.20	20.21-22.02	22.03-23.94	23.95-25.76	25.77-27.42
REL. HUMIDITY (RH) IN FRACTION	0.13-0.19	0.20-0.26	0.27-0.33	0.34-0.41	0.41-0.48

Supplementary Table (2a): Combination matrix for CLUSTER- A

Time Interval	Forest Fire Density (FFD)	Rainfall (R)	Temperature (T)	Relative Humidity (RH)	Solar Radiation (SR)	Favorable Combinations
1-10 March	VL_{FFD}	H_R	M_T	VH_{RH}	VL_{SR}	VL_{FFD}-H_R-M_T-VH_{RH}-VL_{SR}
11-20 March	VL_{FFD}	VH_R	H_T	VH_{RH}	VL_{SR}	VL_{FFD}-VH_R-H_T-VH_{RH}-VL_{SR}
21-30 March	VL_{FFD}	VL_R	H_T	M_{RH}	L_{SR}	VL_{FFD}-VL_R-H_T-M_{RH}-L_{SR}
1-10 April	VL_{FFD}	L_R	H_T	L_{RH}	M_{SR}	VL_{FFD}-L_R-H_T-L_{RH}-M_{SR}
11-20 April	VL_{FFD}	L_R	H_T	L_{RH}	M_{SR}	VL_{FFD}-L_R-H_T-L_{RH}-M_{SR}
21-30 April	VL_{FFD}	M_R	VH_T	L_{RH}	H_{SR}	VL_{FFD}-M_R-VH_T-L_{RH}-H_{SR}
1-10 May	VL_{FFD}	H_R	VH_T	L_{RH}	VH_{SR}	VL_{FFD}-H_R-VH_T-L_{RH}-VH_{SR}

Supplementary Table (2b): Combination matrix for CLUSTER- B

Time Interval	Forest Fire Density (FFD)	Rainfall (R)	Temperature (T)	Relative Humidity (RH)	Solar Radiation (SR)	Favorable Combinations
1-10 March	L_{FFD}	VL_R	H_T	M_{RH}	L_{SR}	L_{FFD}-VL_R-H_T-M_{RH}-L_{SR}
11-20 March	H_{FFD}	H_R	H_T	H_{RH}	L_{SR}	H_{FFD}-H_R-H_T-H_{RH}-L_{SR}
21-30 March	VH_{FFD}	VL_R	H_T	L_{RH}	M_{SR}	VH_{FFD}-VL_R-H_T-L_{RH}-M_{SR}
1-10 April	VH_{FFD}	L_R	H_T	L_{RH}	H_{SR}	VH_{FFD}-L_R-H_T-L_{RH}-H_{SR}
11-20 April	M_{FFD}	L_R	VH_T	L_{RH}	VH_{SR}	M_{FFD}-L_R-VH_T-L_{RH}-VH_{SR}
21-30 April	L_{FFD}	M_R	VH_T	L_{RH}	VH_{SR}	L_{FFD}-M_R-VH_T-L_{RH}-VH_{SR}
1-10 May	VL_{FFD}	H_R	VH_T	VL_{RH}	VH_{SR}	VL_{FFD}-H_R-VH_T-VL_{RH}-VH_{SR}

Supplementary Table (2c): Combination matrix for CLUSTER- C

Time Interval	Forest Fire Density (FFD)	Rainfall (R)	Temperature (T)	Relative Humidity (RH)	Solar Radiation (SR)	Favorable Combinations
1-10 March	VL_{FFD}	M_R	H_T	V_{RH}	VL_{SR}	VL_{FFD}-M_R-H_T-V_{RH}-VL_{SR}
11-20 March	VL_{FFD}	VL_R	H_T	H_{RH}	L_{SR}	VL_{FFD}-VL_R-H_T-H_{RH}-L_{SR}
21-30 March	VL_{FFD}	VL_R	H_T	L_{RH}	M_{SR}	VL_{FFD}-VL_R-H_T-L_{RH}-M_{SR}
1-10 April	VL_{FFD}	VL_R	VH_T	L_{RH}	M_{SR}	VL_{FFD}-VL_R-VH_T-L_{RH}-M_{SR}
11-20 April	VL_{FFD}	VL_R	VH_T	VL_{RH}	H_{SR}	VL_{FFD}-VL_R-VH_T-VL_{RH}-H_{SR}
21-30 April	VL_{FFD}	VL_R	VH_T	VL_{RH}	H_{SR}	VL_{FFD}-VL_R-VH_T-VL_{RH}-H_{SR}
1-10 May	VL_{FFD}	VL_R	VH_T	VL_{RH}	VH_{SR}	VL_{FFD}-VL_R-VH_T-VL_{RH}-VH_{SR}

Supplementary Table (2d): Combination matrix for CLUSTER- D

Time Interval	Forest Fire Density (FFD)	Rainfall (R)	Temperature (T)	Relative Humidity (RH)	Solar Radiation (SR)	Favorable Combinations
1-10 March	VL_{FFD}	H_R	H_T	L_{RH}	L_{SR}	VL_{FFD}-H_R-H_T-L_{RH}-L_{SR}
11-20 March	VL_{FFD}	H_R	H_T	L_{RH}	L_{SR}	VL_{FFD}-H_R-H_T-L_{RH}-L_{SR}
21-30 March	VL_{FFD}	VL_R	H_T	L_{RH}	M_{SR}	VL_{FFD}-VL_R-H_T-L_{RH}-M_{SR}
1-10 April	VL_{FFD}	VL_R	VH_T	L_{RH}	H_{SR}	VL_{FFD}-VL_R-VH_T-L_{RH}-H_{SR}
11-20 April	VL_{FFD}	VL_R	VH_T	VL_{RH}	H_{SR}	VL_{FFD}-VL_R-VH_T-VL_{RH}-H_{SR}
21-30 April	VL_{FFD}	VL_R	VH_T	VL_{RH}	H_{SR}	VL_{FFD}-VL_R-VH_T-VL_{RH}-H_{SR}
1-10 May	VL_{FFD}	VL_R	VH_T	VL_{RH}	H_{SR}	VL_{FFD}-VL_R-VH_T-VL_{RH}-H_{SR}

Supplementary Table (2e): Combination matrix for CLUSTER- E

Time Interval	Forest Fire Density (FFD)	Rainfall (R)	Temperature (T)	Relative Humidity (RH)	Solar Radiation (SR)	Favorable Combinations
1-10 March	VL_{FFD}	M_R	H_T	L_{RH}	L_{SR}	VL_{FFD}-M_R-H_T-L_{RH}-L_{SR}
11-20 March	VL_{FFD}	M_R	H_T	L_{RH}	M_{SR}	VL_{FFD}-M_R-H_T-L_{RH}-M_{SR}
21-30 March	M_{FFD}	VL_R	H_T	L_{RH}	H_{SR}	M_{FFD}-VL_R-H_T-L_{RH}-H_{SR}
1-10 April	H_{FFD}	VL_R	VH_T	L_{RH}	H_{SR}	H_{FFD}-VL_R-VH_T-L_{RH}-H_{SR}
11-20 April	L_{FFD}	VL_R	VH_T	L_{RH}	H_{SR}	L_{FFD}-VL_R-VH_T-L_{RH}-H_{SR}
21-30 April	L_{FFD}	VL_R	VH_T	L_{RH}	H_{SR}	L_{FFD}-VL_R-VH_T-L_{RH}-H_{SR}
1-10 May	VL_{FFD}	VL_R	VH_T	L_{RH}	M_{SR}	VL_{FFD}-VL_R-VH_T-L_{RH}-M_{SR}

Supplementary Table (3): Increment Rate (%) for different variables for period of 11 years (2005-2014). Minus (-) sign before values of different variables in the table indicate decrease in the varialbe during the next consecutive year

Year	Forest Fire	Temperature	Rainfall	Solar Radiation	Relative Humidity
2005	NA	-3.426374905	104.2877569	-2.2960131	4.326826
2006	7.659574	-0.871718159	523.6528193	-3.0640116	26.70147
2007	19.76285	0.505460031	-22.41689945	0.13282665	5.767743
2008	24.09241	1.006416502	-35.04566267	0.98643376	-15.1032
2009	-1.59574	-0.051660685	-28.02045273	0.83970648	10.62269
2010	99.18919	5.0072117	-46.74214497	2.08184676	-6.14426
2011	-73.27	-6.244681383	131.7043009	-2.60473	13.76474
2012	182.7411	0.145352655	-61.399656	3.6691124	-18.9116
2013	-57.4506	0.305466738	-12.47682654	-0.6111587	18.4066
2014	-8.43882	-3.842880329	135.6531656	-1.8054352	9.844333

Summary of OLS Results - Model Variables

Variable	Coefficient [a]	StdError	t-Statistic	robability [b]	Robust_SE	Robust_t	Robust_ r [b]	VIF [c]
Intercept	0.407445	1.553870	0.262213	0.793977	1.259684	0.323450	0.747381	--------
R INF LL	-0.003434	0.004245	-0.808896	0.421477	0.003827	-0.897153	0.372893	3.853155
TEM ER TUR	-0.134798	0.035830	-3.762148	0.000364*	0.045866	-2.938922	0.004535*	4.222561
RH	-3.143155	1.749353	-1.796753	0.076954	1.545358	-2.033933	0.045981*	2.533955
SR	0.242768	0.060527	4.010910	0.000159*	0.083543	2.905903	0.004980*	1.407477

OLS Diagnostics

Input Features:	Dis_wise_Regression_	Dependent Variable:	FFD
Number of Observations:	71	kaike's Information Criterion (ICc) [d]:	-56.101176
Multiple R-Squared [d]:	0.279156	djusted R-Squared [d]:	0.235468
Joint F-Statistic [e]:	6.389834	rob(>F), (4,66) degrees of freedom:	0.000208*
Joint Wald Statistic [e]:	18.088362	rob(>chi-squared), (4) degrees of freedom:	0.001186*
Koenker (B) Statistic [f]:	6.290834	rob(>chi-squared), (4) degrees of freedom:	0.178456
Jarque-Bera Statistic [g]:	83.773048	rob(>chi-squared), (2) degrees of freedom:	0.000000*

Notes on Interpretation

* n asterisk next to a number indicates a statistically significant p-value (p < 0.01).

[a] Coefficient: Represents the strength and type of relationship between each explanatory variable and the dependent variable.

[b] robability and Robust robability (Robust_ r): sterisk (*) indicates a coefficient is statistically significant (p < 0.01); if the Koenker (B) Statistic [f] is statistically significant, use the Robust robability column (Robust_ r) to determine coefficient significance.

[c] Variance Inflation Factor (VIF): Large Variance Inflation Factor (VIF) values (> 7.5) indicate redundancy among explanatory variables.

[d] R-Squared and kaike's Information Criterion (ICc): Measures of model fit/performance.

[e] Joint F and Wald Statistics: sterisk (*) indicates overall model significance (p < 0.01); if the Koenker (B) Statistic [f] is statistically significant, use the Wald Statistic to determine overall model significance.

[f] Koenker (B) Statistic: When this test is statistically significant (p < 0.01), the relationships modeled are not consistent (either due to non-stationarity or heteroskedasticity). You should rely on the Robust robabilities (Robust_ r) to determine coefficient significance and on the Wald Statistic to determine overall model significance.

[g] Jarque-Bera Statistic: When this test is statistically significant (p < 0.01) model predictions are biased (the residuals are not normally distributed).

Variable Distributions and Relationships

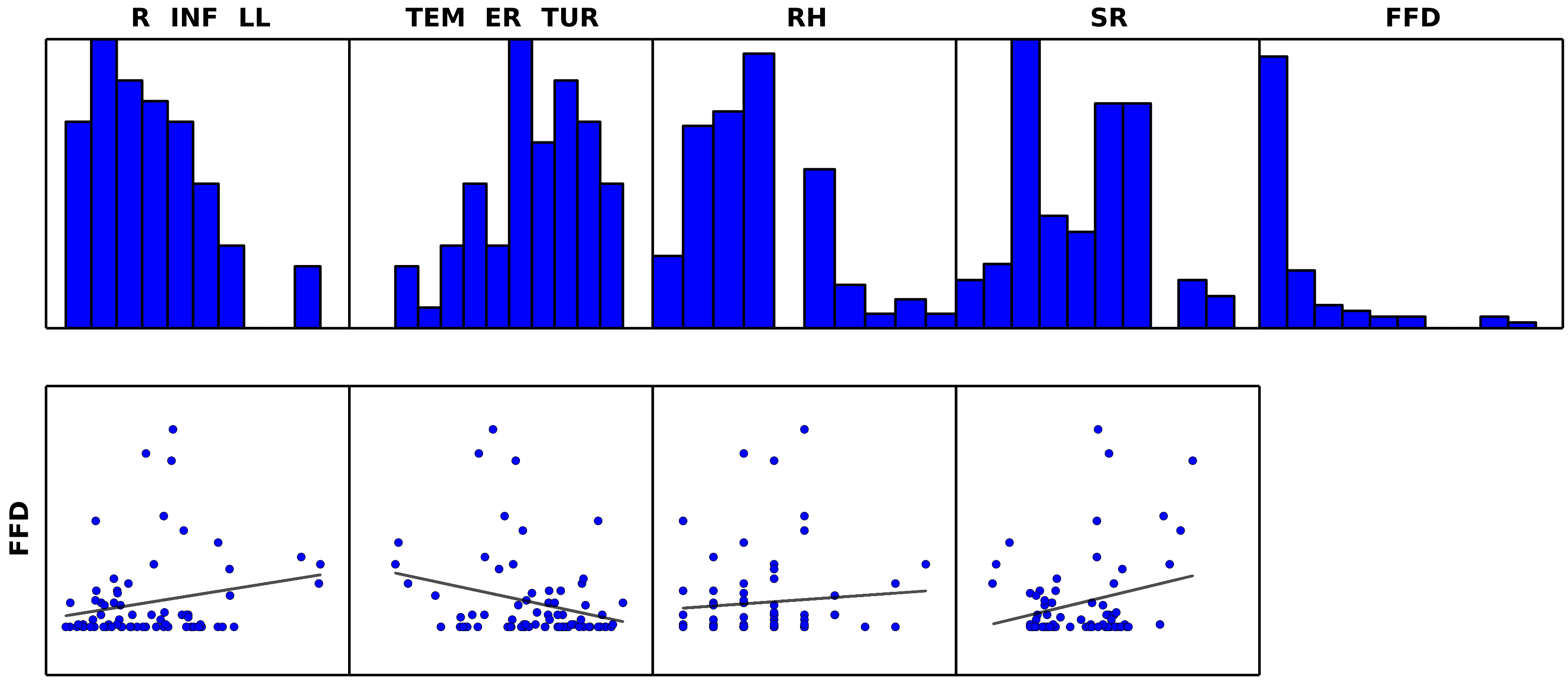

The above graphs are Histograms and Scatterplots for each explanatory variable and the dependent variable. The histograms show how each variable is distributed. OLS does not require variables to be normally distributed. However, if you are having trouble finding a properly-specified model, you can try transforming strongly skewed variables to see if you get a better result.

Each scatterplot depicts the relationship between an explanatory variable and the dependent variable. Strong relationships appear as diagonals and the direction of the slant indicates if the relationship is positive or negative. Try transforming your variables if you detect any non-linear relationships. For more information see the Regression nalysis Basics documentation.

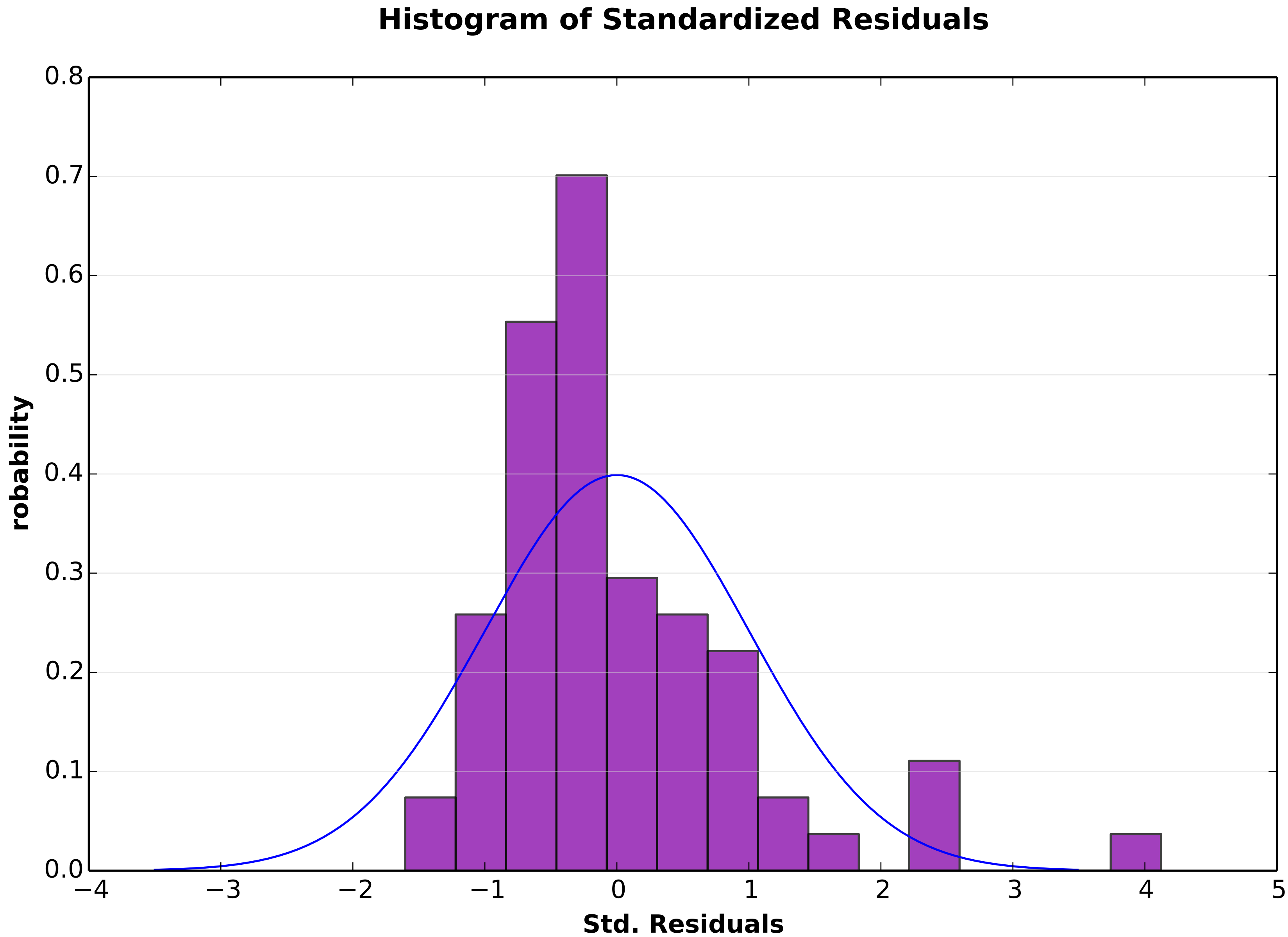

Ideally the histogram of your residuals would match the normal curve, indicated above in blue. If the histogram looks very different from the normal curve, you may have a biased model. If this bias is significant it will also be represented by a statistically significant Jarque-Bera p-value (*).

Residual vs.   redicted   lot

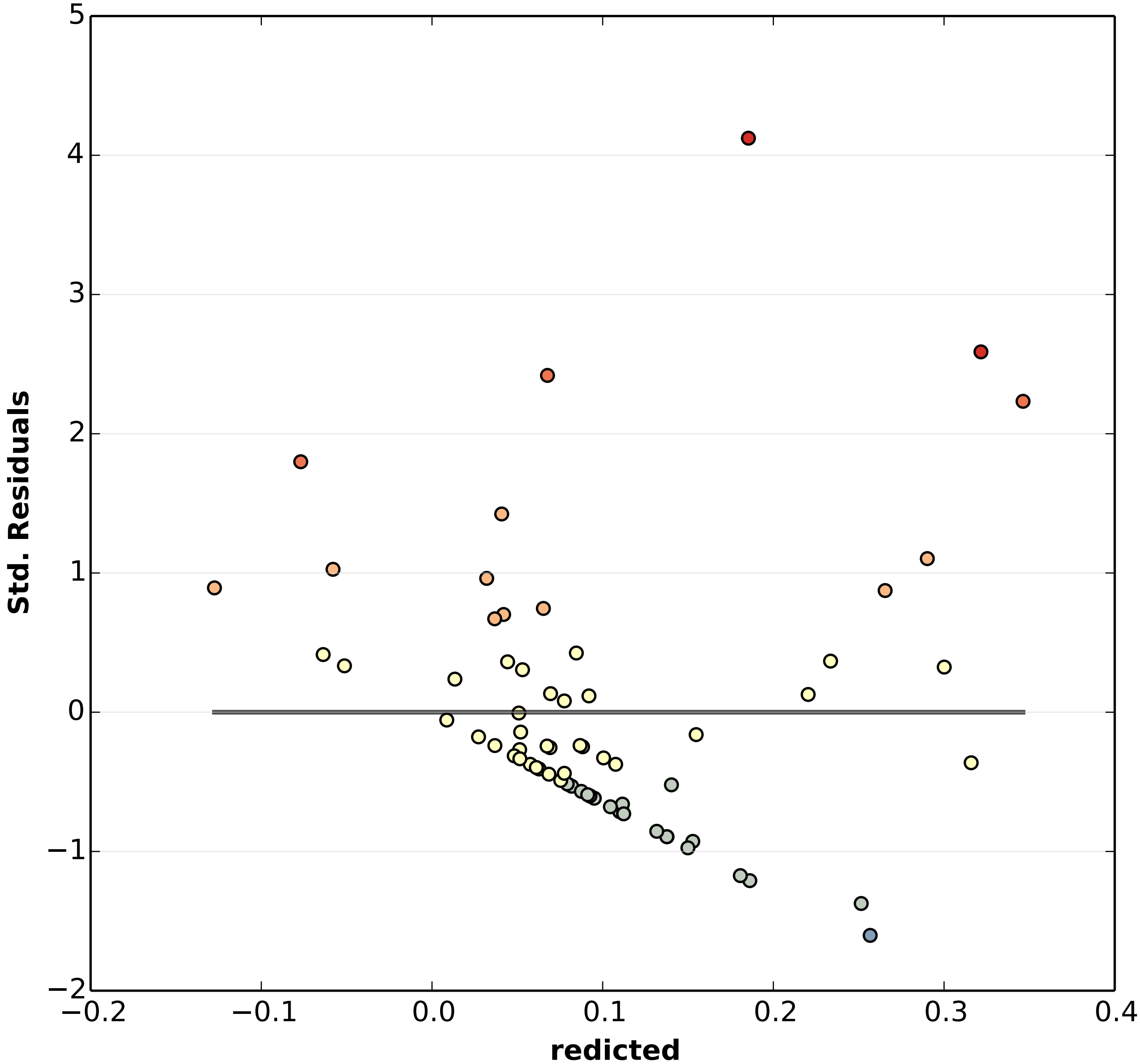

This is a graph of residuals (model over and under predictions) in relation to predicted dependent variable values. For a properly specified model, this scatterplot will have little structure, and look random (see graph on the right). If there is a structure to this plot, the type of structure may be a valuable clue to help you figure out what's going on.

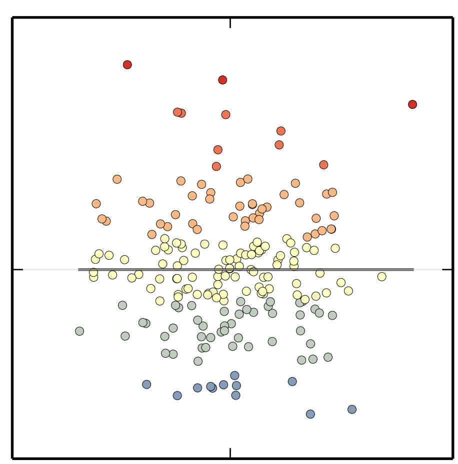

Random Residuals

Ordinary Least Squares arameters

arameter Name	Input Value
Input Features	Dis_wise_Regression_
Unique ID Field	UID
Output Feature Class	None
Dependent Variable	FFD
Explanatory Variables	R INF LL
	TEM ER TUR
	RH
	SR
Selection Set	False

Spatial Autocorrelation Report

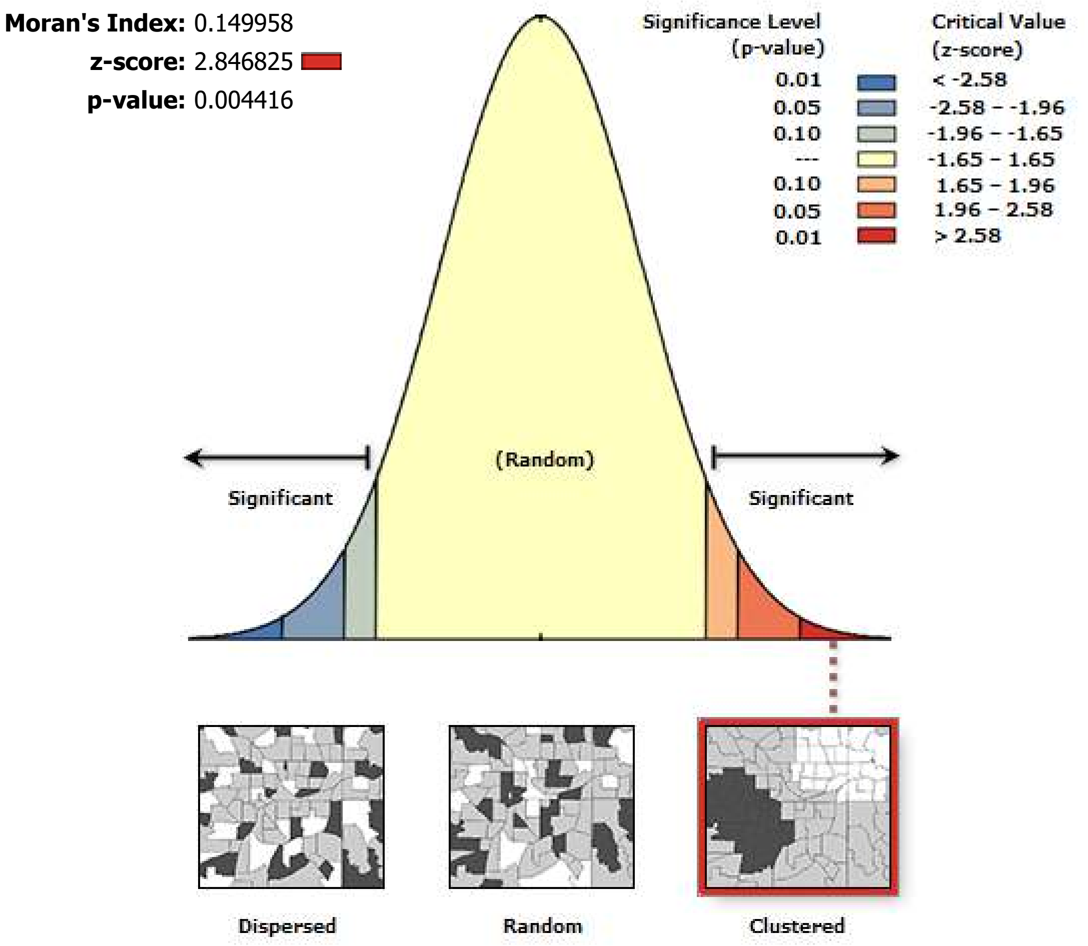

Given the z-score of 2.84682533156, there is a less than 1% likelihood that this clustered pattern could be the result of random chance.

Global Moran's I Summary

Moran's Index:	0.149958
Expected Index:	-0.014286
Variance:	0.003329
z-score:	2.846825
p-value:	0.004416

Dataset Information

Input Feature Class:	Dis_wise_Regression_P_OLS
Input Field:	RESIDUAL
Conceptualization:	INVERSE_DISTANCE
Distance Method:	EUCLIDEAN

Row Standardization:	False
Distance Threshold:	106653.4705 Meters
Weights Matrix File:	None
Selection Set:	False